Instabilities for a relativistic electron beam interacting with a laser-irradiated plasma

Hrachya B. Nersisyan[1,2,*] and Claude Deutsch[3,†]
[1]*Institute of Radiophysics and Electronics, 0203 Ashtarak, Armenia*
[2]*Centre of Strong Fields Physics, Yerevan State University, 0025 Yerevan, Armenia*
[3]*LPGP (UMR-CNRS 8578), Université Paris XI, 91405 Orsay, France*
(Received 25 March 2012; published 29 May 2012)

The effects of a radiation field (RF) on the unstable modes developed in a relativistic electron beam-plasma interaction are investigated assuming that $\omega_0 > \omega_p$, where ω_0 is the frequency of the RF and ω_p is the plasma frequency. These unstable modes are parametrically coupled to each other due to the RF and are a mix between two-stream and parametric instabilities. The dispersion equations are derived by the linearization of the kinetic equations for a beam-plasma system as well as the Maxwell equations. In order to highlight the effect of the radiation field we present a comparison of our analytical and numerical results obtained for nonzero RF with those for vanishing RF. Assuming that the drift velocity $\mathbf{u}_b$ of the beam is parallel to the wave vector $\mathbf{k}$ of the excitations two particular transversal and parallel configurations of the polarization vector $\mathbf{E}_0$ of the RF with respect to $\mathbf{k}$ are considered in detail. It is shown that in both geometries resonant and nonresonant couplings between different modes are possible. The largest growth rates are expected at the transversal configuration when $\mathbf{E}_0$ is perpendicular to $\mathbf{k}$. In this case it is demonstrated that, in general, the spectrum of the unstable modes in the ω-k plane is split into two distinct domains with long and short wavelengths, where the unstable modes are mainly sensitive to the beam or the RF parameters, respectively. In the parallel configuration, $\mathbf{E}_0 \parallel \mathbf{k}$, and at short wavelengths the growth rates of the unstable modes are sensitive to both beam and RF parameters remaining insensitive to the RF at long wavelengths.

DOI: 10.1103/PhysRevE.85.056414 PACS number(s): 52.40.Mj, 52.40.Db, 52.35.Mw, 52.35.Qz

I. INTRODUCTION

The interaction of a relativistic electron beam (REB) with a plasma is a subject of relevance for many fields of physics, ranging from inertial fusion to astrophysics [1–5]. This interaction is also relevant, among others, for the fast ignition scenario (FIS) [6,7], where the precompressed deuterium-tritium (DT) core of a fusion target is to be ignited by a laser-generated relativistic electron beam. The REB quickly prompts a return current so one eventually has to deal with a typical two-stream configuration which is subjected to various electromagnetic instabilities. Much effort has been devoted in the past few years to investigate these instabilities [8–21], whether it is the two-stream [22,23], the filamentation [24], or Weibel [25] instabilities. These instabilities are usually analyzed by linearizing the relativistic Vlasov or fluid and Maxwell equations. The response of the linearized equation to a perturbation then is investigated and one eventually finds some unstable self-excited modes. At this stage, the orientation of the wave vector $\mathbf{k}$ of the excitations plays an important role. Choosing a wave vector parallel to the beam velocity $\mathbf{u}_b$ yields the two-stream unstable modes which are of electrostatic nature and therefore characterized by wave and electric field vectors both parallel to the beam propagation direction. On the other hand, choosing a wave vector normal to the beam yields the purely transverse filamentation unstable modes. They are mostly electromagnetic, purely growing, and develop preferentially in the plane normal to the beam. The exploration of the much less investigated intermediate orientations has brought a very important result by showing that the strongest instability suffered by the system is eventually to be found for an oblique wave vector [14–20,26,27]. This most unstable mode is a mixture of the two-stream and the filamentation instabilities but it is not damped as the last two ones. For example, the maximum two-stream growth rate is reduced by a factor of γ^{-1} in the relativistic regime, while the most unstable mode only decreases by a factor of $\gamma^{-1/3}$, where γ is the beam relativistic factor. The filamentation growth rate varies as $\gamma^{-1/2}$ and may be reduced, even canceled, by a transverse beam temperature [12], whereas the most unstable mode is quite insensitive to temperatures as long as they are nonrelativistic [15].

In general beam-plasma instabilities have been studied in detail for many physical situations, including the interaction of the cold, warm, inhomogeneous, or anisotropic electron or ion beams with cold, warm, magnetized, unmagnetized, inhomogeneous, or anisotropic plasmas; see, e.g., Refs. [8–21] and references therein (see also Refs. [28,29] for detailed bibliography). In this paper, we present a study of the effects of a radiation field (RF) on the interaction of REB with a plasma. More specifically, our objective is to study the beam-plasma instabilities in a laser-irradiated plasma which, to our knowledge, has not been discussed in the literature. The principal motivation of the present paper is the research on the topic of the FIS for inertial confinement fusion [6,7] which involves the interaction of a laser-generated REB with a hot plasma. Although the concept of the FIS implies an overdense plasma and the propagation of a relativistic electron beam from the border of a precompressed target to the dense core occurs without crossing the laser beam, the target plasma is assumed to be parametrically excited by the RF through high-harmonics generation. In addition, a promising inertial confinement fusion scheme has been recently proposed [30–32], in which the plasma target is irradiated simultaneously by intense laser

*hrachya@irphe.am
†claude.deutsch@pgp.u-psud.fr

and ion beams. In both situations, the presence of the RF can dramatically change the main features of the standard (i.e., when the laser is off) beam-plasma instabilities.

Previously, the interaction of charged particles with plasma in the presence of the RF has been a subject of great activity in the contexts of the stopping power [33–36] (see also references therein) and other processes of interest for applications in optics, solid-state, and fusion research. In particular, the analytical calculations [33–35] as well as the particle-in-cell (PIC) numerical simulations [36] show that the propagation and the subsequent stopping of the charged particles would be essentially affected by the parametric excitations of the plasma target by means of laser irradiation. It is well known that, in general, in the absence of the charged-particle beams the laser-irradiated plasma is subjected to the parametric instabilities [37,38]. Therefore, in the present context it is expected that the above-mentioned beam-plasma unstable modes developed in a plasma irradiated simultaneously by laser and electron beams are parametrically coupled to each other and are not, in principle, distinguishable.

The plan of the paper is as follows. In Sec. II, we outline the kinetic formulation for the interaction of the REB with a laser-irradiated plasma. The full electromagnetic response of the plasma is considered. The general linear dispersion relations are derived in Sec. III, which are studied for two particular cases in Secs. IV and V with transversal and parallel configurations of the polarization vector of the RF with respect to $\mathbf{k}$, respectively. Furthermore, assuming nonrelativistic laser intensities, only the lowest (zero, first, and second) harmonics of the electromagnetic fields are considered. The obtained dispersion equations are investigated numerically in Sec. VI. The results are summarized in Sec. VII, which also includes discussion and outlook. In Appendix A we consider the standard (in the absence of the RF) stable and unstable modes of the beam-plasma system in a cold-fluid approximation. The asymptotic behavior of the frequencies and the growth rates of these modes at large and small k are considered. In Appendix B, we provide some technical details for an evaluation of the sum containing Bessel functions. An equation describing the evolution of the amplitude of the parametrically excited plasma waves and involving all excited harmonics is derived and discussed in Appendix C. Throughout, the Gaussian units are used unless otherwise indicated.

II. THEORETICAL BACKGROUND

In this section, we consider the main aspects of the interaction of the relativistic electron beam (REB) with a homogeneous, collisionless, and unmagnetized plasma in the presence of high-frequency radiation field (RF), $\mathbf{E}_0(t) = \mathbf{E}_0 \sin(\omega_0 t)$. Here $\mathbf{E}_0$ and ω_0 are the amplitude and the frequency of the RF. The problem is formulated using the perturbative treatment and includes the effects of the RF in a self-consistent way. The RF is treated in the long-wavelength limit, and the plasma particles (electrons and ions) are considered nonrelativistic. These are good approximations provided that (1) the wavelength of the RF ($\lambda_0 = 2\pi c/\omega_0$) is much larger than the Debye screening length $\lambda_D = v_{\rm th}/\omega_p$, with $v_{\rm th}$ the thermal velocity of the electrons and ω_p the plasma frequency, and (2) the "quiver velocity" of the electrons in the RF ($v_E = eE_0/m\omega_0$) is much smaller than the speed of light c. These conditions can be alternatively written as (1) $\omega_0/\omega_p \ll 2\pi c/v_{\rm th}$ and (2) $I_L \ll \frac{1}{2}n_e mc^3(\omega_0/\omega_p)^2$, where $I_L = cE_0^2/8\pi$ is the RF intensity. As an estimate in the case of dense plasma, with electron density $n_e = 10^{23}$ cm^{-3}, we get $\frac{1}{2}n_e mc^3 \simeq 1.2 \times 10^{20}$ W/cm^2. Thus, the limits (1) and (2) are well above the values obtained with currently available high-power RF sources, and so the approximations are well justified. Furthermore, we consider an underdense plasma with $\omega_0 > \omega_p$.

The dynamics of the beam-plasma system is governed by the relativistic and nonrelativistic Vlasov kinetic equations for the distribution functions of the REB $f_b(\mathbf{r},\mathbf{v},t)$ and the plasma $f_\alpha(\mathbf{r},\mathbf{v},t)$ (where $\alpha = e,i$ indicates the plasma species), respectively, as well as by the Maxwell equations for the electromagnetic fields. Thus,

$$\frac{\partial f_{\alpha,b}}{\partial t} + \mathbf{v}\cdot\frac{\partial f_{\alpha,b}}{\partial \mathbf{r}} + e_{\alpha,b}\left\{\mathbf{E}_0(t) + \mathbf{E} + \frac{1}{c}[\mathbf{v}\times\mathbf{B}]\right\}\cdot\frac{\partial f_{\alpha,b}}{\partial \mathbf{p}} = 0, \tag{1}$$

where e_α and e_b are the charges of the plasma and beam particles, respectively, and $\mathbf{E}$ and $\mathbf{B}$ are the self-consistent electromagnetic fields which are determined by the Maxwell equations,

$$\nabla\times\mathbf{E} = -\frac{1}{c}\frac{\partial \mathbf{B}}{\partial t}, \quad \nabla\times\mathbf{B} = \frac{4\pi}{c}\left(\sum_\alpha \mathbf{j}_\alpha + \mathbf{j}_b\right) + \frac{1}{c}\frac{\partial \mathbf{E}}{\partial t}, \tag{2}$$

$$\nabla\cdot\mathbf{E} = 4\pi\left(\sum_\alpha e_\alpha n_\alpha + e_b n_b\right), \quad \nabla\cdot\mathbf{B} = 0. \tag{3}$$

Here $n_\alpha(\mathbf{r},t)$ and $n_b(\mathbf{r},t)$ are the densities for the plasma species α and for the relativistic beam, respectively, and $\mathbf{j}_\alpha(\mathbf{r},t)$ and $\mathbf{j}_b(\mathbf{r},t)$ are the corresponding currents induced in plasma and beam, respectively,

$$\begin{aligned} n_{\alpha,b}(\mathbf{r},t) &= \int f_{\alpha,b}(\mathbf{r},\mathbf{p},t)d\mathbf{p}, \\ \mathbf{j}_{\alpha,b}(\mathbf{r},t) &= e_{\alpha,b}\int \mathbf{v} f_{\alpha,b}(\mathbf{r},\mathbf{p},t)d\mathbf{p}. \end{aligned} \tag{4}$$

As mentioned above we consider a nonrelativistic plasma and in Eq. (1) for the distribution function f_α the momentum connects linearly to the particle velocity, $\mathbf{p} = m_\alpha\mathbf{v}$, where m_α is the mass of the plasma species α. Equation (1) for the distribution function f_b is relativistic and $\mathbf{p} = m_b\gamma\mathbf{v}$ in this case, where $\gamma = (1 - v^2/c^2)^{-1/2}$ and m_b are the relativistic factor and the rest mass of the beam particles. Moreover, we consider an ultrarelativistic electron beam with $\gamma_b = (1 - u_b^2/c^2)^{-1/2} \gg 1$, where u_b is the beam drift velocity, and, therefore, the influence of the RF $\mathbf{E}_0(t)$ on the beam is ignored in the kinetic equation (1) for the distribution function $f_b(\mathbf{r},\mathbf{p},t)$.

For sufficiently small perturbations, we assume $f_{\alpha,b} = f_{0\alpha,b} + f_{1\alpha,b}$ (with $f_{1\alpha,b} \ll f_{0\alpha,b}$), where $f_{0\alpha}$ and f_{0b} are the equilibrium distribution functions of the plasma species α and the beam in an unperturbed state, respectively. The solution of the linearized kinetic equation (1) for the relativistic beam, when the RF $\mathbf{E}_0(t)$ in Eq. (1) is neglected, is well known.

This standard calculation is explained at length in a number of plasma physics textbooks [38–41], and we just here mention the final result. In terms of the Fourier-transformed quantities, the solution of the kinetic equation reads

$$f_{1b}(\mathbf{k},\omega,\mathbf{p}) = ie_b E_j(\mathbf{k},\omega)\left[\delta_{ij}\left(1-\frac{k_s v_s}{\omega}\right)+\frac{k_i v_j}{\omega}\right] \times \frac{\partial f_{0b}(\mathbf{p})}{\partial p_i}\frac{1}{\mathbf{k}\cdot\mathbf{v}-\omega-i0}. \quad (5)$$

Here $\mathbf{E}(\mathbf{k},\omega)$ and $f_{1b}(\mathbf{k},\omega,\mathbf{p})$ are the Fourier transforms of the electric field and the beam distribution function, respectively, with respect to variables $\mathbf{r}$ and t, δ_{ij} is the unit tensor of rank 3. Note that the positive infinitesimal $+i0$ in Eq. (5) guarantees the causality of the response.

The perturbations of the densities and the currents induced in the plasma and the beam are determined from Eq. (4). The Fourier transforms of these quantities are then given by

$$n_{1\alpha,b}(\mathbf{k},\omega) = \int f_{1\alpha,b}(\mathbf{k},\omega,\mathbf{p})d\mathbf{p}, \qquad \mathbf{j}_{1\alpha,b}(\mathbf{k},\omega) = e_{\alpha,b}\int \mathbf{v} f_{1\alpha,b}(\mathbf{k},\omega,\mathbf{p})d\mathbf{p}. \quad (6)$$

Substituting the distribution function (5) into these quantities and integrating by parts with the help of the relation $\partial v_i/\partial p_j = (1/m_b\gamma)(\delta_{ij} - v_i v_j/c^2)$ [where $\gamma^2(p) = 1 + p^2/m_b^2c^2$] for the induced current and the density of the beam we obtain

$$j_{1b,i}(\mathbf{k},\omega) = \sigma_{b,ij}(\mathbf{k},\omega)E_j(\mathbf{k},\omega), \quad (7)$$

$$e_b n_{1b}(\mathbf{k},\omega) = \frac{ie_b^2}{m_b\omega}\mathbf{E}(\mathbf{k},\omega)\cdot\int\left[\mathbf{k}+\mathbf{v}\frac{k^2-(\mathbf{k}\cdot\mathbf{v})\omega/c^2}{\omega-\mathbf{k}\cdot\mathbf{v}+i0}\right] \times \frac{f_{0b}(\mathbf{p})d\mathbf{p}}{\gamma(p)(\omega-\mathbf{k}\cdot\mathbf{v}+i0)}, \quad (8)$$

where $\sigma_{b,ij}(\mathbf{k},\omega)$ is the conductivity tensor of the relativistic charged-particle beam,

$$\sigma_{b,ij}(\mathbf{k},\omega) = \frac{ie_b^2}{m_b\omega}\int\left[\delta_{ij}+\frac{v_i k_j + k_i v_j}{\omega-\mathbf{k}\cdot\mathbf{v}+i0} + v_i v_j\frac{k^2-\omega^2/c^2}{(\omega-\mathbf{k}\cdot\mathbf{v}+i0)^2}\right]\frac{f_{0b}(\mathbf{p})d\mathbf{p}}{\gamma(p)}. \quad (9)$$

Consider now the solution of the kinetic equation (1) for the plasma electrons and ions in the presence of the high-frequency RF. In an unperturbed state (i.e., neglecting the self-consistent electromagnetic fields $\mathbf{E}$ and $\mathbf{B}$ in Eq. (1) and assuming the homogeneous initial state) the distribution function satisfies the equation

$$\frac{\partial f_{0\alpha}}{\partial t} + e_\alpha \mathbf{E}_0\sin(\omega_0 t)\cdot\frac{\partial f_{0\alpha}}{\partial \mathbf{p}} = 0, \quad (10)$$

which yields the equilibrium distribution function for the plasma species α,

$$f_{0\alpha}(\mathbf{p},t) = F_\alpha[\mathbf{p}+m_\alpha\mathbf{v}_{E\alpha}\cos(\omega_0 t)]. \quad (11)$$

Here $F_\alpha(\mathbf{p})$ is an arbitrary function. Below we will assume that this function is isotropic in momentum space. $\mathbf{v}_{E\alpha} = e_\alpha\mathbf{E}_0/m_\alpha\omega_0$ and $\mathbf{a}_\alpha = e_\alpha\mathbf{E}_0/m_\alpha\omega_0^2$ are the quiver velocity and the oscillation amplitude of the plasma species α, respectively, driven by the RF.

Next we consider the linearized kinetic equation for the plasma species α. Introducing the Fourier transforms $f_{1\alpha}(\mathbf{k},\mathbf{p},t)$, $\mathbf{E}(\mathbf{k},t)$, and $\mathbf{B}(\mathbf{k},t)$ with respect to the coordinate $\mathbf{r}$, the linearized kinetic equation reads

$$\left[\frac{\partial}{\partial t} + i(\mathbf{k}\cdot\mathbf{v}) + e_\alpha\mathbf{E}_0\sin(\omega_0 t)\cdot\frac{\partial}{\partial\mathbf{p}}\right]f_{1\alpha}(\mathbf{k},\mathbf{p},t) = -e_\alpha\left[\mathbf{E}(\mathbf{k},t)+\frac{1}{c}[\mathbf{v}\times\mathbf{B}(\mathbf{k},t)]\right]\cdot\frac{\partial f_{0\alpha}}{\partial\mathbf{p}}. \quad (12)$$

In order to solve Eq. (12) it is convenient to introduce a new unknown function Ψ_α via relation

$$f_{1\alpha}(\mathbf{k},\mathbf{p},t) = e^{i\zeta_\alpha\sin(\omega_0 t)}\Psi_\alpha(\mathbf{k},\mathbf{P},t), \quad (13)$$

where $\zeta_\alpha = (\mathbf{k}\cdot\mathbf{a}_\alpha)$ and $\mathbf{P} = \mathbf{p} + m_\alpha\mathbf{v}_{E\alpha}\cos(\omega_0 t)$. Substituting this relation into Eq. (12) it is easy to see that the obtained equation for the unknown function Ψ_α constitutes an equation with periodic coefficients where the role of the dynamic momentum is now played by the quantity $\mathbf{P}$. Therefore, we introduce the decomposition

$$Q(\mathbf{k},\mathbf{p},t) = \int_{-\infty}^{\infty}d\omega e^{-i\omega t}\sum_{n=-\infty}^{\infty}Q^{(n)}(\mathbf{k},\omega,\mathbf{p})e^{-in\omega_0 t}, \quad (14)$$

where $Q(\mathbf{k},\mathbf{p},t)$ represents one of the quantities $\Psi_\alpha(\mathbf{k},\mathbf{p},t)$, $\mathbf{E}(\mathbf{k},t)$, and $\mathbf{B}(\mathbf{k},t)$ and $Q^{(n)}(\mathbf{k},\omega,\mathbf{p})$ is the corresponding amplitude of the nth harmonic. From Maxwell equation we express the magnetic field through the electric field. In terms of the amplitudes of the nth harmonics [see definition given by Eq. (14)] this relation is given by

$$\mathbf{B}^{(n)}(\mathbf{k},\omega) = \frac{c}{\omega+n\omega_0}[\mathbf{k}\times\mathbf{E}^{(n)}(\mathbf{k},\omega)]. \quad (15)$$

Also in the kinetic equation derived for $\Psi_\alpha^{(n)}$ the term $[k_i v_j - \delta_{ij}(\mathbf{k}\cdot\mathbf{v})](\partial F_\alpha/\partial p_i) = 0$ vanishes due to the isotropy of the equilibrium distribution function F_α of the plasma particles. Thus, using the Fourier series representation of the exponential function [42] [see also Eq. (C2)] for the amplitude of the nth harmonic of the distribution function, we finally obtain

$$\Psi_\alpha^{(n)}(\mathbf{k},\omega,\mathbf{p}) = -\frac{ie_\alpha}{\omega+n\omega_0-\mathbf{k}\cdot\mathbf{v}+i0}\frac{\partial F_\alpha(\mathbf{p})}{\partial p_i} \times\sum_{\ell=-\infty}^{\infty}J_{n-\ell}(\zeta_\alpha)\left[\delta_{ij}+\frac{(n-\ell)\omega_0}{\omega+\ell\omega_0}\left(\delta_{ij}-\frac{k_i a_{\alpha,j}}{\zeta_\alpha}\right)\right] \times E_j^{(\ell)}(\mathbf{k},\omega). \quad (16)$$

Here J_n is the Bessel function of the nth order. Throughout this paper the upper indices given in the parentheses indicate the harmonic number while the lower indices determine the components of the vectors and tensors.

The amplitudes of the harmonics of the induced current and the charge density in a plasma are obtained from Eqs. (6), (13), (14), and (16). Straightforward calculations

yield

$$j_r^{(s)}(\mathbf{k},\omega) = \sum_{\ell=-\infty}^{\infty} \sigma_{rj}^{(s\ell)}(\mathbf{k},\omega) E_j^{(\ell)}(\mathbf{k},\omega), \tag{17}$$

$$e_\alpha n_\alpha^{(s)}(\mathbf{k},\omega) = -\frac{ik}{4\pi} \sum_{n=-\infty}^{\infty} J_{n-s}(\zeta_\alpha)\delta\varepsilon_{\alpha\parallel}(n) \sum_{\ell=-\infty}^{\infty} \frac{\omega + n\omega_0}{\omega + \ell\omega_0} \times J_{n-\ell}(\zeta_\alpha)[\boldsymbol{\chi}^{(\ell n)}(\mathbf{k},\omega)\cdot \mathbf{E}^{(\ell)}(\mathbf{k},\omega)] \tag{18}$$

for the Fourier transforms of the sth harmonics of the current and the charge density, respectively, with

$$\boldsymbol{\chi}^{(\ell n)}(\mathbf{k},\omega) = \frac{\mathbf{k}}{k} + \frac{(\ell - n)\omega_0}{\omega + n\omega_0}\frac{k}{\zeta_\alpha}\mathbf{a}_\alpha. \tag{19}$$

Here we have introduced the conductivity tensor $\sigma_{rj}^{(s\ell)}(\mathbf{k},\omega)$

$$\sigma_{rj}^{(s\ell)}(\mathbf{k},\omega) = \frac{1}{4\pi i}\sum_\alpha \sum_{n=-\infty}^{\infty} \frac{(\omega + n\omega_0)^2}{\omega + \ell\omega_0} J_{n-\ell}(\zeta_\alpha) J_{n-s}(\zeta_\alpha) \times \left[\left(\delta_{jr} - \frac{k_j k_r}{k^2}\right)\delta\varepsilon_{\alpha\perp}(n) + \chi_j^{(\ell n)}(\mathbf{k},\omega)\chi_r^{(sn)}(\mathbf{k},\omega)\delta\varepsilon_{\alpha\parallel}(n)\right] \tag{20}$$

and the abbreviations $\delta\varepsilon_{\alpha\parallel;\perp}(n) \equiv \delta\varepsilon_{\alpha\parallel;\perp}(k,\omega + n\omega_0)$, where $\delta\varepsilon_{\alpha\parallel}(k,\omega)$ and $\delta\varepsilon_{\alpha\perp}(k,\omega)$ are the partial contributions of the plasma species α to the longitudinal and transversal (with respect to the wave vector $\mathbf{k}$) dielectric functions (see, e.g., Ref. [39]), respectively,

$$\delta\varepsilon_{\alpha\parallel}(k,\omega) = \frac{4\pi e_\alpha^2}{k^2} k_i \int \frac{\partial F_\alpha(\mathbf{p})}{\partial p_i}\frac{d\mathbf{p}}{\omega - \mathbf{k}\cdot\mathbf{v} + i0}, \tag{21}$$

$$\delta\varepsilon_{\alpha\perp}(k,\omega) = \frac{2\pi e_\alpha^2}{\omega}\int \left[v_i - \frac{(\mathbf{k}\cdot\mathbf{v})k_i}{k^2}\right]\frac{\partial F_\alpha(\mathbf{p})}{\partial p_i} \times \frac{d\mathbf{p}}{\omega - \mathbf{k}\cdot\mathbf{v} + i0}. \tag{22}$$

Note that since the equilibrium distribution function F_α is isotropic, the partial dielectric functions $\delta\varepsilon_{\alpha\parallel;\perp}(k,\omega)$ are also isotropic, i.e., they do not depend on the direction of the wave vector $\mathbf{k}$. The obtained expressions (17)–(22) with Eqs. (7)–(9) as well as the Maxwell equations (2) and (3) written in the Fourier space completely determine the electromagnetic response in the beam-plasma system in the presence of the RF. Using this system of equations the general dispersion equations are derived in the next section.

We would like to close this section with the following two remarks. First, the distribution function $f_{1b}(\mathbf{k},\omega,\mathbf{p})$ of the beam particles given by Eq. (5) as well as the induced current (7) and the charge density (8) are determined by the Fourier transform $\mathbf{E}(\mathbf{k},\omega)$ of the electric field. In contrast to this case, the distribution function [Eq. (13) with Eqs. (14) and (16)], the induced current [Eq. (17)] and the density [Eq. (18)] of the plasma are determined by the Fourier transform of the amplitude of the harmonics of the electric field, $\mathbf{E}^{(n)}(\mathbf{k},\omega)$. From Eq. (14) it is straightforward to deduce the connection between the Fourier transforms $\mathbf{E}(\mathbf{k},\omega)$ and $\mathbf{E}^{(n)}(\mathbf{k},\omega)$. Changing the integration variable in each term of summation in Eq. (14) according to $\omega + n\omega_0 \to \omega$, we obtain

$$\mathbf{E}(\mathbf{k},\omega) = \sum_{n=-\infty}^{\infty} \mathbf{E}^{(n)}(\mathbf{k},\omega - n\omega_0). \tag{23}$$

Thus, $\mathbf{E}(\mathbf{k},\omega)$ is the sum of all harmonics $\mathbf{E}^{(n)}(\mathbf{k},\omega)$ with shifted frequencies $\omega \pm n\omega_0$. Second, assuming an ultrarelativistic beam for derivation of the distribution function (5) we have neglected the RF in the kinetic equation (1) for f_b. And as a consequence, the perturbation of the beam distribution function is determined by $\mathbf{E}(\mathbf{k},\omega)$. Although the RF is not directly involved in the kinetic equation (1) for f_b, it affects this distribution function via the self-consistent electric field $\mathbf{E}(\mathbf{k},\omega)$ containing all harmonics produced by the RF [see Eq. (23)].

III. DISPERSION EQUATION

In this section, using the expressions derived for the induced currents in the beam and plasma, we consider the dispersion equation of the waves excited in a plasma by the relativistic beam of charged particles. For this purpose, we employ the Maxwell equations (2). Introducing Fourier transforms of the electric field and the currents according to Eq. (14), and excluding the magnetic field from these equations by means of Eq. (15) from Eqs. (2), (7)–(9), and (17)–(20) for the components of the amplitude of the nth harmonic of the electric field, we obtain

$$\left\{\delta_{rj}\left[k^2 - \frac{(\omega + n\omega_0)^2}{c^2}\right] - k_r k_j\right\} E_j^{(n)}(\mathbf{k},\omega) = \frac{4\pi i(\omega + n\omega_0)}{c^2}\left[\sum_{\ell=-\infty}^{\infty}\sigma_{rj}^{(n\ell)}(\mathbf{k},\omega)E_j^{(\ell)}(\mathbf{k},\omega) + \delta_{n0}\sigma_{b,rj}(\mathbf{k},\omega)E_j(\mathbf{k},\omega)\right]. \tag{24}$$

Here the conductivity tensors of the plasma $\sigma_{rj}^{(n\ell)}(\mathbf{k},\omega)$ and the beam $\sigma_{b,rj}(\mathbf{k},\omega)$ are determined by Eqs. (20) and (9), respectively. It is seen that, in the right-hand side of Eq. (24), the beam current vanishes for any nonzero harmonic number, $n \neq 0$.

Before starting the systematic investigation of the general dispersion equation for the beam-plasma system in the presence of the RF it is constructive consider briefly two limiting cases of Eq. (24). First, at the vanishing RF (i.e., at $\zeta_\alpha \to 0$) from Eq. (20), it is straightforward to calculate the conductivity tensor $\sigma_{ij}^{(n\ell)}(\mathbf{k},\omega)$ of the plasma, which reads, in this limit,

$$\sigma_{ij}^{(n\ell)}(\mathbf{k},\omega) = \delta_{n\ell}\frac{\omega + n\omega_0}{4\pi i}[\varepsilon_{ij}(n) - \delta_{ij}] \equiv \delta_{n\ell}\sigma_{ij}(n). \tag{25}$$

Here we have introduced (as above) the abbreviations $\sigma_{ij}(n) \equiv \sigma_{ij}(\mathbf{k},\omega + n\omega_0)$, $\varepsilon_{ij}(n) \equiv \varepsilon_{ij}(\mathbf{k},\omega + n\omega_0)$, $\varepsilon_{\parallel;\perp}(n) \equiv \varepsilon_{\parallel;\perp}(k,\omega + n\omega_0)$ and $\sigma_{ij}(\mathbf{k},\omega)$ and

$$\varepsilon_{ij}(\mathbf{k},\omega) = \frac{k_i k_j}{k^2}\varepsilon_\parallel(k,\omega) + \left(\delta_{ij} - \frac{k_i k_j}{k^2}\right)\varepsilon_\perp(k,\omega) \tag{26}$$

are the conductivity and the dielectric tensors of an isotropic plasma, respectively, with longitudinal $[\varepsilon_\parallel(k,\omega)]$ and transversal $[\varepsilon_\perp(k,\omega)]$ dielectric functions (see, e.g.,

Refs. [38,39]),

$$\varepsilon_{\parallel,\perp}(k,\omega) = 1 + \sum_{\alpha} \delta\varepsilon_{\alpha\parallel,\perp}(k,\omega). \tag{27}$$

Substituting Eq. (25) into Eq. (24), we obtain that $E_j^{(n)}(\mathbf{k},\omega) = \delta_{n0} E_j(\mathbf{k},\omega)$ and Eq. (23) is fulfilled automatically. Thus, after some simplifications, we arrive at

$$\left\{k^2\delta_{ij} - k_i k_j - \frac{\omega^2}{c^2}[\varepsilon_{ij}(\mathbf{k},\omega) + \delta\varepsilon_{b,ij}(\mathbf{k},\omega)]\right\} E_j(\mathbf{k},\omega) = 0. \tag{28}$$

Here $\varepsilon_{ij}(\mathbf{k},\omega) + \delta\varepsilon_{b,ij}(\mathbf{k},\omega)$ is the total dielectric tensor of the beam-plasma system, where $\delta\varepsilon_{b,ij}(\mathbf{k},\omega) = (4\pi i/\omega)\sigma_{b,ij}(\mathbf{k},\omega)$ is the partial contribution of the beam to the total dielectric tensor of the system. Equating the determinant of the system of linear equations (28) to zero yields the general dispersion equation for the beam-plasma system. In the past few years this equation has been studied in detail for arbitrary orientation of the electron beam propagation direction with respect to the wave vector $\mathbf{k}$; see, e.g., Refs. [10–21]. In particular, assuming a cold, homogeneous, and monochromatic charged-particle beam with an unperturbed distribution function $f_{0b}(\mathbf{p}) = n_b\delta(\mathbf{p} - \mathbf{p}_b)$, where n_b is the beam density, from Eq. (9) one obtains

$$\delta\varepsilon_{b,ij}(\mathbf{k},\omega) = -\frac{\omega_b^2}{\gamma_b\omega^2}\left[\delta_{ij} + \frac{u_{bi}k_j + u_{bj}k_i}{\omega - \mathbf{k}\cdot\mathbf{u}_b} + \frac{u_{bi}u_{bj}(k^2 - \omega^2/c^2)}{(\omega - \mathbf{k}\cdot\mathbf{u}_b)^2}\right]. \tag{29}$$

Here $\mathbf{p}_b = m_b\gamma_b\mathbf{u}_b$, $\gamma_b = (1 - u_b^2/c^2)^{-1/2}$, and $\omega_b^2 = 4\pi n_b e_b^2/m_b$ are the relativistic factor and the plasma frequency of the beam, respectively. At this stage it is convenient to represent the vectors (particularly the electric field) in the form of an expansion in the components parallel, $A_\parallel = (\mathbf{k}\cdot\mathbf{A})/k$, and perpendicular, $\mathbf{A}_\perp = \mathbf{A} - (\mathbf{k}/k)A_\parallel$, to the wave vector $\mathbf{k}$. In particular, choosing a wave vector $\mathbf{k}$ parallel to the beam velocity $\mathbf{u}_b$ yields the two-stream (TS) unstable modes which are of electrostatic nature with $E_\parallel(\mathbf{k},\omega) \neq 0$ and $\mathbf{E}_\perp(\mathbf{k},\omega) = 0$. Introducing the longitudinal dielectric function of the beam by means of the relation

$$\delta\varepsilon_{b\parallel}(\mathbf{k},\omega) = \frac{k_i k_j}{k^2}\delta\varepsilon_{b,ij}(\mathbf{k},\omega) = -\frac{\omega_b^2}{\gamma_b^3(\omega - k u_{b\parallel})^2}, \tag{30}$$

the dispersion equation in this case for a beam-plasma system then reads

$$\mathcal{D}_\parallel(k,\omega) \equiv \varepsilon_\parallel(k,\omega) + \delta\varepsilon_{b\parallel}(k,\omega) = 0. \tag{31}$$

On the other hand, choosing $\mathbf{k}$ normal to the beam velocity $\mathbf{u}_b$ yields the purely transverse (electromagnetic) filamentation unstable modes. It should be emphasized that we have considered above an infinite beam of charged particles and, as a consequence, the plasma return current is not involved in Eqs. (29)–(31) in self-consistent manner. This is not, however, a strong limitation of the present treatment. For instance, the drift velocity $\mathbf{u}_e$ of the plasma return flow can be deduced from the beam current neutralization condition, $n_e\mathbf{u}_e \simeq -n_b\mathbf{u}_b$. Then, within a cold-fluid model, the return current is included by adding into Eqs. (29) and (30) the similar terms but with a flow velocity $\mathbf{u}_e$ and plasma density n_e [14–16].

Second, in the case of the absence of the external beam, the last term in the right-hand side of Eq. (24) vanishes. The remaining infinite system of equations for the electric field harmonics then represents the electromagnetic response of the plasma to the RF. In general, the longitudinal and transversal components of the electric field are coupled parametrically and the excitations are a mixture of both types of modes. Previously, the parametrically unstable modes have been studied in detail both for the electrostatic [43] (see also Refs. [37,38]) and electromagnetic [44,45] excitations. The purely electrostatic excitations with $\mathbf{E}_\perp^{(\ell)} = 0$ are possible when the polarization vector of the laser radiation is parallel to the wave vector $\mathbf{k}$ ($\mathbf{E}_{0\perp} = 0$). In this case, the plasma electrons and ions are driven by the laser field only in the direction of $\mathbf{k}$.

To illustrate the problem of the charged-particle beam-plasma instabilities developed in a laser-irradiated plasma, we consider below two examples when the polarization vector $\mathbf{E}_0$ of the RF is perpendicular (Sec. IV) or parallel (Sec. V) to the wave vector $\mathbf{k}$. We consider an infinite and cold beam of charged particles of velocity $\mathbf{u}_b$ aligned with the direction of $\mathbf{k}$ and uniform density n_b passing through a homogeneous electron plasma with density of electrons n_e. Therefore, the partial contribution of the beam to the total dielectric function of the beam-plasma system is given by Eq. (29). For simplicity, we will use throughout the notation $u_{b\parallel} = u_b$ for the beam velocity. In the case the RF is off the chosen geometry corresponds to the excitations of the TS unstable modes provided that the return plasma current is included in the dispersion relations. Nevertheless, in the present study neglecting the return current we will adopt the terminology "two-stream instability." This should not be confusing as long as the velocity of the beam is parallel to $\mathbf{k}$.

IV. TRANSVERSAL POLARIZATION OF THE RF ($\mathbf{E}_0 \perp \mathbf{k}$)

In this section we consider Eq. (24) for the harmonics of the electric field when the polarization vector $\mathbf{E}_0$ of the laser field is perpendicular to $\mathbf{k}$ [$(\mathbf{k}\cdot\mathbf{E}_0) = 0$ and $\zeta_\alpha = 0$]. From Eq. (20) it then is seen that the nonvanishing components of the conductivity tensor are $\sigma_{rj}^{(\ell,\ell)}$, $\sigma_{rj}^{(\ell,\ell\pm1)}$, $\sigma_{rj}^{(\ell,\ell\pm2)} \neq 0$ while $\sigma_{rj}^{(\ell,\ell\pm p)} = 0$ at $p \geqslant 3$. Using this fact Eq. (24) for the electric field harmonics is represented as

$$\left[k^2\delta_{rj} - k_r k_j - \frac{(\omega + \ell\omega_0)^2}{c^2}\Sigma_{rj}(\ell)\right]E_j^{(\ell)}(0) = D_{rj}^{+}(\ell)E_j^{(\ell+1)}(0) + D_{rj}^{-}(\ell)E_j^{(\ell-1)}(0) + R_{rj}^{+}(\ell)E_j^{(\ell+2)}(0) + R_{rj}^{-}(\ell)E_j^{(\ell-2)}(0) + \frac{\omega^2}{c^2}\delta_{\ell0}\delta\varepsilon_{b,rj}(\mathbf{k},\omega)E_j(0), \tag{32}$$

where we have introduced the following notations: $\mathbf{E}^{(n)}(\ell) \equiv \mathbf{E}^{(n)}(\mathbf{k},\omega - \ell\omega_0)$, $\mathbf{E}(\ell) \equiv \mathbf{E}(\mathbf{k},\omega - \ell\omega_0)$, $\Sigma_{rj}(\ell) \equiv \Sigma_{rj}(\mathbf{k},\omega + \ell\omega_0)$, $D_{rj}^{\pm}(\ell) \equiv D_{rj}^{\pm}(\mathbf{k},\omega + \ell\omega_0)$, $R_{rj}^{\pm}(\ell) \equiv R_{rj}^{\pm}(\mathbf{k},\omega + \ell\omega_0)$, $\delta\varepsilon_{b,rj}(\ell) \equiv \delta\varepsilon_{b,rj}(\mathbf{k},\omega + \ell\omega_0)$, and

$$\Sigma_{rj}(\mathbf{k},\omega) = \varepsilon_{rj}(\mathbf{k},\omega) + \frac{k^2\omega_0^2}{4\omega^2}\sum_{\alpha} a_{\alpha r}a_{\alpha j} \times [\delta\varepsilon_{\alpha\parallel}(-1) + \delta\varepsilon_{\alpha\parallel}(1)], \tag{33}$$

$$D_{rj}^{\pm}(\mathbf{k},\omega) = -\frac{\omega_0\omega}{2c^2}\sum_{\alpha}\left[\frac{\omega}{\omega\pm\omega_0}k_r a_{\alpha j}\delta\varepsilon_{\alpha\parallel}(0) + k_j a_{\alpha r}\delta\varepsilon_{\alpha\parallel}(\pm 1)\right], \tag{34}$$

$$R_{rj}^{\pm}(\mathbf{k},\omega) = \frac{k^2\omega_0^2}{4c^2}\frac{\omega}{\omega\pm 2\omega_0}\sum_{\alpha} a_{\alpha r}a_{\alpha j}\delta\varepsilon_{\alpha\parallel}(\pm 1). \tag{35}$$

In the following we consider throughout an electron plasma neglecting the dynamics of plasma ions. Thus we restrict ourself by the frequency domain well above the ionic frequencies. We introduce the oscillation amplitude and the quiver velocity of the electrons via relations $\mathbf{a}_e = -a\mathbf{e}$, $\mathbf{v}_{Ee} = -v_E\mathbf{e}$, $v_E = eE_0/m\omega_0$, $a = eE_0/m\omega_0^2$ ($-e$ is the electron charge), and $\mathbf{e} = \mathbf{E}_0/E_0$. So the quantities a and v_E are positive by definition.

Next, for the exclusion of harmonics $E_j^{(\ell)}(0)$ in Eq. (32), the frequency ω is replaced by $\omega - \ell\omega_0$ and, using Eq. (23), we perform summation over ℓ. This yields an equation for the amplitude $E_j(0)$ of the electric field,

$$\left[k^2\delta_{rj} - k_r k_j - \frac{\omega^2}{c^2}\Sigma_{rj}(0)\right]E_j(0) = D_{rj}^{+}(0)E_j(-1) + D_{rj}^{-}(0)E_j(1) + R_{rj}^{+}(0)E_j(-2) + R_{rj}^{-}(0)E_j(2) + \frac{\omega^2}{c^2}\delta\varepsilon_{b,rj}(0)E_j(0). \tag{36}$$

The resulting equation represents an infinite system of linear equations for the quantities $E_j(\pm p)$ (with $p = 0,1,2,\ldots$). The (infinite) determinant of this system determines the dispersion equation for the beam-plasma system in the presence of the RF.

It follows from Eq. (36) that, for the perturbations of which electric vector $\mathbf{E}(0)$ is polarized perpendicular to the plane of the vectors $\mathbf{k}$ and $\mathbf{E}_0$, there is no instability. The dispersion equation for these modes is given by $\mathcal{D}_\perp(k,\omega) = 0$, where

$$\mathcal{D}_\perp(k,\omega) = 1 + \frac{1}{k^2c^2}\left[\frac{\omega_b^2}{\gamma_b} - \omega^2\varepsilon_\perp(k,\omega)\right]. \tag{37}$$

This is simply the dispersion equation for the ordinary transverse electromagnetic modes propagating in an isotropic plasma [38,39] in the absence of the RF but modified due to the presence of the beam. The second term in the right-hand side of Eq. (37) with the minus sign is the partial contribution of the transverse dielectric function of a cold beam to the total transverse dielectric function of the beam-plasma system. It is noteworthy that this contribution depends on γ_b^{-1} while the longitudinal contribution (30) decays as γ_b^{-3} with the beam relativistic factor.

To reveal the instability we consider, therefore, the case of a polarization wherein the electric vector $\mathbf{E}(0)$ of the perturbations lies in the plane containing the vectors $\mathbf{k}$ and $\mathbf{E}_0$. Introducing the components of the electric field parallel ($E_\parallel$) and perpendicular ($\mathbf{E}_\perp$) to the wave vector $\mathbf{k}$, for these modes from Eq. (36), we obtain

$$\mathcal{D}_\parallel(0)E_\parallel(0) = -\frac{kv_E}{2}[\psi(1) + \psi(-1)]\delta\varepsilon_\parallel(0), \tag{38}$$

$$\left\{\mathcal{D}_\perp(0) - \frac{v_E^2}{4c^2}[\delta\varepsilon_\parallel(1) + \delta\varepsilon_\parallel(-1)]\right\}\psi(0) = \frac{v_E^2}{4c^2}[\psi(-2)\delta\varepsilon_\parallel(1) + \psi(2)\delta\varepsilon_\parallel(-1)] + \frac{v_E}{2kc^2}[E_\parallel(-1)\delta\varepsilon_\parallel(1) + E_\parallel(1)\delta\varepsilon_\parallel(-1)], \tag{39}$$

where $\mathcal{D}_\parallel(\ell) \equiv \mathcal{D}_\parallel(k,\omega+\ell\omega_0)$, $\mathcal{D}_\perp(\ell) \equiv \mathcal{D}_\perp(k,\omega+\ell\omega_0)$, and $\psi(\mathbf{k},\omega) = [\mathbf{e}\cdot\mathbf{E}_\perp(\mathbf{k},\omega)]/\omega$ with $\psi(\ell) \equiv \psi(\mathbf{k},\omega-\ell\omega_0)$. Let us recall that the function $\mathcal{D}_\parallel(0)$ given by Eq. (31) is the total longitudinal dielectric function of the beam-plasma system in the absence of the RF. In this case, the transverse and longitudinal modes are independent with the dispersion relations $\mathcal{D}_\perp(0) = 0$ and $\mathcal{D}_\parallel(0) = 0$, respectively. However, in the presence of the laser radiation these modes are parametrically coupled according to Eqs. (38) and (39). The longitudinal electric fields in Eq. (39) can be excluded inserting the values $E_\parallel(-1)$ and $E_\parallel(1)$ calculated by means of Eq. (38) into Eq. (39). The given equation then contains only the harmonics $\psi(0)$ and $\psi(\pm 2)$. Similarly, the transverse fields can be partially excluded from Eq. (38), evaluating the harmonics $\psi(1)$ and $\psi(-1)$ by means of Eq. (39). In this case, Eq. (38) cannot be decoupled completely since it involves not only the longitudinal electric fields but also the higher harmonics of the transverse fields. Also, it should be noted that the nonlinear response of the system is accompanied by the magnetic-field generation according to Eq. (15). It follows from this equation that the magnetic field is directed perpendicularly to the plane containing the vectors $\mathbf{k}$ and $\mathbf{E}_0$.

In principle, the dispersion equations of the perturbations can be deduced from Eqs. (38) and (39) by solving these equations by iteration to any order of accuracy. However, taking into account the smallness of the parameter v_E/c, it suffices to restrict the analysis of the system (38) and (39) to the harmonics $E_\parallel(0)$, $E_\parallel(\pm 2)$, and $\psi(0)$, $\psi(\pm 2)$. In this case, the longitudinal and transversal modes are decoupled and we obtain the following dispersion equations:

$$\mathcal{D}_\parallel(k,\omega) + \frac{v_E^2}{4c^2}\left[\frac{1}{\mathcal{D}_\perp(k,\omega-\omega_0)} + \frac{1}{\mathcal{D}_\perp(k,\omega+\omega_0)}\right]\times\delta\varepsilon_\parallel^2(k,\omega) = 0, \tag{40}$$

$$\mathcal{D}_\perp(k,\omega) = \frac{v_E^2}{4c^2}\sum_{\nu=\pm}\frac{\delta\varepsilon_\parallel(k,\omega+\nu\omega_0)\varepsilon_{b\parallel}(k,\omega+\nu\omega_0)}{\mathcal{D}_\parallel(k,\omega+\nu\omega_0)}, \tag{41}$$

for longitudinal and transversal modes, respectively. Here $\varepsilon_{b\parallel}(k,\omega) = 1 + \delta\varepsilon_{b\parallel}(k,\omega)$.

A. Longitudinal modes

Let us now investigate the dispersion equations (40) and (41) in detail within the fluid model (or the cold plasma approximation) when the partial dielectric functions are given by

$$\delta\varepsilon_\perp(k,\omega) = \delta\varepsilon_\parallel(k,\omega) \equiv \delta\varepsilon(\omega) = -\frac{\omega_p^2}{\omega^2}. \tag{42}$$

Here $\omega_p^2 = 4\pi n_e e^2/m$ is the plasma frequency. Thus, we consider only the high-frequency modes assuming that $|\omega| \gg k v_{\rm th}$, where $v_{\rm th}$ is the thermal velocity of the electrons. We look for the solutions of the dispersion equations in the form $\omega = \omega_r + i\gamma$, where ω_r is the (real) frequency and γ is the damping rate (when $\gamma < 0$) or the growth rate (when $\gamma > 0$) of the modes, respectively. In the absence of the laser field ($v_E = 0$), the transverse modes are stable and their frequency is determined by

$$\omega_\perp^2(k) = k^2c^2 + \frac{\omega_b^2}{\gamma_b} + \omega_p^2. \tag{43}$$

It is seen that the frequency of the ordinary transverse modes is modified by the charged-particle beam effectively increasing the total plasma frequency of the beam-plasma system. Also, it should be noted that the contribution of the beam to the dispersion relation of the transverse modes is $\sim\omega_b^2/\gamma_b$ while for the longitudinal modes it is given by $\sim\omega_b^2/\gamma_b^3$ [see, e.g., Eq. (30)]. This is a consequence of the anisotropy of the effective electron mass with respect to the driving force acting either in the longitudinal or transversal directions. The stability of the mode (43) can be easily understood taking into account the fact that the electric field vector in this mode is perpendicular to the beam and, hence, the work performed by this field on the beam particles is zero.

The longitudinal two-stream modes are unstable in a long-wavelength regime (see, e.g., Ref. [28]) with $0 \leqslant k \leqslant k_c \equiv \omega_c/u_b$, where $\omega_c = \omega_p(1+\xi^{1/3}/\gamma_b)^{3/2}$ and $\xi = \omega_b^2/\omega_p^2$. Note that, in practice, $\xi \ll 1$ and $\omega_c \simeq \omega_p$. Assuming that $k \ll k_c$, the growth rate and the frequency of the two-stream modes read [cf. with Eqs. (A4) and (A5)]

$$\gamma^{\rm TS}(k) \simeq k u_b \frac{\left(\xi/\gamma_b^3\right)^{1/2}}{1+\xi/\gamma_b^3}, \quad \omega_\parallel^{\rm TS}(k) \simeq \frac{k u_b}{1+\xi/\gamma_b^3}, \tag{44}$$

respectively. It is seen that the real frequency of the TS modes $\simeq k u_b$, i.e., it is a frequency-locked oscillation, the frequency depending only the Čherenkov-type term and not on the natural frequency of the oscillations ($\sim\omega_p$). The maximal value of $\gamma^{\rm TS}(k)$ is achieved at $k \lesssim k_c$ [28] and is given by

$$\frac{\gamma_{\rm max}^{\rm TS}}{\omega_p} \simeq \frac{\sqrt{3}}{2^{4/3}}\frac{\xi^{1/3}}{\gamma_b}. \tag{45}$$

In the presence of the laser field ($v_E \neq 0$), the high-frequency transversal and the low-frequency longitudinal modes, Eqs. (43) and (44) and then (45), respectively, of the beam-plasma system are parametrically coupled according to Eqs. (40) and (41). These equations can be satisfied only when one of the ordinary dispersion functions $\mathcal{D}_\parallel(k,\omega)$ or $\mathcal{D}_\perp(k,\omega)$, becomes nearly equal to zero. This is not, however, sufficient to cause parametric TS instability, which occurs when at least two of the zeros of the dispersion functions merge, as in the case of the standard TS instability [28,38]. In the case of the longitudinal waves, there are three such situations: (i) Čherenkov-type coupling when $\omega_r \simeq k u_b$; (ii) $\mathcal{D}_\parallel(k,\omega) \simeq 0$ and $\mathcal{D}_\perp(k,\omega \pm \omega_0) \simeq 0$; (iii) $\mathcal{D}_\perp(k,\omega + \omega_0) \simeq 0$ and $\mathcal{D}_\perp(k,\omega - \omega_0) \simeq 0$. Cases (i) and (ii) correspond to the resonant coupling, and case (iii) corresponds to the nonresonant coupling.

Consider the situation (i) which corresponds to the low-frequency [$\omega \sim \omega_\parallel^{\rm TS}(k)$], long-wavelength excitations. Close to the Čherenkov resonance, $\omega \simeq k u_b$, the most important term in Eq. (40) is involved in $\delta\varepsilon_{b\parallel}(\mathbf{k},\omega)$ [Eq. (30)]. Consequently, we look for the solution of the dispersion equation (40) in the form $\omega = k u_b + \omega_1$, where $|\omega_1| \ll k u_b$. In this case, the instability occurs at $k u_b \lesssim \omega_s \sim \omega_p$ with the growth rate ($\omega_1 = i\gamma$) [cf. with Eq. (44)]

$$\gamma(k) \simeq \left(\frac{\xi}{\gamma_b^3}\right)^{1/2} \frac{k u_b}{\sqrt{F(k u_b)}}, \tag{46}$$

where ω_s is the zero of the function $F(\omega)$, $F(\omega_s) = 0$, and

$$F(\omega) = 1 - \frac{\omega^2}{\omega_p^2} - \frac{v_E^2}{4c^2}\frac{\omega_p^2}{\omega^2} \times \left[\frac{1}{\mathcal{D}_\perp(k,\omega-\omega_0)} + \frac{1}{\mathcal{D}_\perp(k,\omega+\omega_0)}\right]. \tag{47}$$

It is noteworthy that the root k_0 of the transversal dispersion function, $\mathcal{D}_\perp(k,\omega-\omega_0) \simeq 0$ with $\omega = k u_b$, at $\omega_0 \lesssim 2\omega_p$ may lie in the domain $k u_b \lesssim \omega_s$ and the growth rate (46) changes the slope close to this root. At $k \gtrsim k_0$ the function $F(\omega)$ becomes negative and the relation (46) is violated. However, at $\omega_0 \gtrsim 2\omega_p$ the formula (46) remains valid in the whole domain of the instability. Also, the maximal growth rate is achieved at $k u_b \simeq \omega_s$. Equation (46) is clearly invalid in this case and more rigorous treatment of the dispersion equation yields

$$\gamma_{\rm max} \simeq \frac{\sqrt{3}}{2^{4/3}}\left[\frac{\xi}{\gamma_b^3}\frac{2\omega_s^2}{|F'(\omega_s)|}\right]^{1/3}. \tag{48}$$

Here the prime indicates the derivative of the function with respect to the argument.

We have considered above the low-frequency and long-wavelength regime when the dispersion properties of the system are strongly determined by the beam characteristics (density and the energy). Next we consider the high-frequency [$\omega > \omega_\parallel^{\rm TS}(k)$], short-wavelength regime with $k u_b \gtrsim \omega_s$. This case corresponds to the situations (ii) and (iii) introduced above. Assuming a low-density beam with $n_b \ll n_e$, we note that the role of the beam in the dispersion properties of the system becomes less pronounced in this high-frequency regime, and, as a first approximation, the terms proportional to ω_b^2 can be neglected in Eq. (40). This is a regime of purely parametric excitations in a plasma.

The resonant coupling (ii) occurs when the following resonance condition is satisfied:

$$\omega_0 \simeq \omega_p + \omega_\perp(k). \tag{49}$$

In either case, $|\omega|$ is assumed to be much smaller than ω_0 and $\omega_\perp(k)$. We can then make the resonance approximation for the dispersion function $\mathcal{D}_\perp(k,\omega \pm \omega_0)$ to obtain

$$\mathcal{D}_\perp(k,\omega \pm \omega_0) \simeq \mp\frac{1}{k^2c^2}(2\omega_0 - \delta)(\omega \pm \delta), \tag{50}$$

where $\delta(k) = \omega_0 - \omega_\perp(k)$ is the mismatch of the laser frequency from the frequency of the natural transversal mode. Substituting Eq. (50) into (40) and neglecting the contribution of the beam in the dispersion relation of the left-hand side of

Eq. (40) yields a cubic equation for ω^2,

$$\omega^2\left(\omega^2-\omega_p^2\right)\left(\omega^2-\delta^2\right)+\frac{k^2v_E^2}{4}\frac{\omega_p^4\delta}{\omega_0-\delta/2}=0, \quad (51)$$

which can be solved analytically. However, we restrict ourself to the simple and qualitative solutions of the dispersion equation and more rigorous numerical calculations will be presented in Sec. VI.

As mentioned above, there are two types of solutions of the high-frequency [$\omega > \omega_\parallel^{\mathrm{TS}}(k)$] dispersion equation (51). First, we consider the resonant solution assuming that $\delta \simeq \omega_p > 0$. Note that this type of instability resembles the resonant decay instability. The sum frequency of the excited modes is exactly equal to the laser frequency ω_0 [see Eq. (49)]. Introducing the frequency mismatch $\Delta(k) = \delta(k) - \omega_p$ ($\Delta \ll \omega_p$, δ), the dispersion equation (51) for the resonant growth rate yields

$$\gamma_r(k) = \tfrac{1}{2}\sqrt{\epsilon^2k^2c^2-\Delta^2(k)}, \quad (52)$$

where $\epsilon = (v_E/2c)(\tau-1/2)^{-1/2}$, $\tau = \omega_0/\omega_p$. The resonant unstable mode exists only at $\tau \gtrsim 2$. The maximal growth rate $\gamma_{r,\max}$ is achieved at $k = k_{r,\max}$ with

$$k_{r,\max} = \frac{\omega_p}{c}\frac{\sqrt{(\tau-2+\epsilon^2)(\tau-\epsilon^2)}}{1-\epsilon^2}, \quad (53)$$

$$\gamma_{r,\max} = \frac{\omega_p}{2}\epsilon\sqrt{\frac{\tau(\tau-2)+\epsilon^2}{1-\epsilon^2}}. \quad (54)$$

Now, in this high-frequency domain, the characteristics of the instability are only weakly sensitive to the beam density and energy (γ_b) but essentially depend on the laser intensity and the frequency. It is seen that the maximal growth rate is scaled as (at $\tau \gg 1$) $\gamma_{r,\max} \sim [I_L(\omega_p/\omega_0)]^{1/2}$, where I_L is the RF intensity. It is also noteworthy that at $\tau \gg 1$ the position $k_{r,\max}$ of the maximum of the resonant growth rate is independent on the laser intensity ($k_{r,\max} \simeq \omega_0/c$). Equations (52)–(54) can be compared with the growth rate of the ordinary two-stream instability, Eq. (45). Assuming, for simplicity, a high-frequency laser field ($\omega_0 \gg \omega_p$), one obtains that, at $v_E/c > \sqrt{3/\tau}(4\xi/\gamma_b^3)^{1/3}$, the growth rate $\gamma_{r,\max}$ exceeds $\gamma_{\max}^{\mathrm{TS}}$. Note that the last inequality is easily fulfilled for the REB.

In the nonresonant case (iii), assuming that $|\omega| \ll \omega_p$ from Eq. (51), one obtains a quadratic equation for ω^2. A simple analysis of this equation shows that, in this case, the instability occurs at $-\delta_m \leqslant \delta \leqslant \omega_0 - \omega_p$, where $\delta_m = \omega_p[2\epsilon_1(kc/\omega_p)]^{2/3}$ with $\epsilon_1 = (v_E/2c)(\tau-\delta/2\omega_p)^{-1/2}$. Two distinct branches of the instability should be considered separately. At the positive frequency mismatch, $0 \leqslant \delta \leqslant \omega_0 - \omega_p$ [or $k \leqslant k_2 \equiv (\omega_p/c)(\tau^2-1)^{1/2}$], the instability is almost aperiodic (i.e., $\omega_r \simeq 0$) with the growth rate

$$\gamma = \frac{\delta^{1/4}}{\sqrt{2}}\left(\sqrt{\delta^3+\delta_m^3}-\delta^{3/2}\right)^{1/2}, \quad (55)$$

while at the negative values with $-\delta_m \leqslant \delta \leqslant 0$ ($k_2 \leqslant k \leqslant k_1$, where $\delta = -\delta_m$ at $k = k_1$), the instability is periodic (i.e., $\omega_r \neq 0$) and the growth rate becomes

$$\gamma = \frac{|\delta|^{1/4}}{2}(\delta_m^{3/2}-|\delta|^{3/2})^{1/2}. \quad (56)$$

The real frequency of the unstable mode (56) is obtained by changing the minus sign in this formula by a plus sign. We note that the latter nonresonant case with $\delta < 0$ resembles the oscillating two-stream instability.

Thus, summarizing this section, we emphasize that, in the spectrum of the longitudinal unstable modes, there are basically three domains with strictly different properties. The "long wavelength" domain with $k \lesssim \omega_p/u_b$ (we denote this parameter regime as Domain I) is basically determined by the beam density and the energy (γ_b) and corresponds to the TS instability [see, e.g., Eqs. (45) and (46)]. The intermediate (Domain II, $k \leqslant k_2$) and the short-wavelength (Domain III, $k_2 \leqslant k \leqslant k_1$) regimes mainly depend on the laser intensity and are only weakly sensitive to the beam parameters. In Domains II and III the growth rates can be approximated by Eqs. (55) and (56), respectively. In addition, in Domain II at $\omega_0 \gtrsim 2\omega_p$, it is possible to witness a resonant excitation of the unstable modes with maximal growth rate (54) which resembles the resonant decay instability. Finally, Domain I may merge to Domain II at $k \simeq \omega_p/u_b$ while Domain II merges to Domain III at the zero-frequency mismatch, $\delta = 0$ ($k = k_2$).

B. Transversal modes

In this section we turn to the investigation of the unstable transversal modes generated in the beam-plasma system. Our starting point is the dispersion equation (41) for these modes. As in Sec. IV A, we adopt here a cold-fluid approximation when the partial dielectric functions of the beam and the plasma are given by Eqs. (30) and (42), respectively. An inspection of the dispersion equation (41) shows that there is only one resonant coupling between different modes. This is the situation when $\mathcal{D}_\perp(k,\omega) \simeq 0$ and $\mathcal{D}_\parallel(k,\omega-\omega_0) \simeq 0$. This system of equations require that $\omega \simeq \omega_0 + \omega_s(k) + \Delta\omega(k)$ and $\omega_\perp(k) \simeq \omega_0 + \omega_s(k)$, where $\Delta\omega \ll \omega_0 + \omega_s$, $\omega_\perp(k)$ is the frequency of the ordinary transversal modes, Eq. (43), and ω_s is the real root of the ordinary dispersion equation, $\mathcal{D}_\parallel(k,\omega_s) = 0$, for the longitudinal modes. Note that the resonant condition $\omega_\perp \simeq \omega_0 + \omega_s$ cannot be satisfied in the domain where the two-stream instability occurs, where $\omega_s(k) = \omega_\parallel^{\mathrm{TS}}(k) + i\gamma^{\mathrm{TS}}(k)$ [see, e.g., Eqs. (44) and (45)] is a complex quantity. Therefore, it is expected that the resonance occurs at short wavelengths ($k \gtrsim k_c$) and at high frequencies ($\omega \gtrsim \omega_\parallel^{\mathrm{TS}}(k)$)). Inserting $\omega \simeq \omega_0 + \omega_s + \Delta\omega$ and $\omega_\perp \simeq \omega_0 + \omega_s$ into Eq. (41) and neglecting a small term depending on the frequency $\omega + \omega_0$ in the right-hand side of this equation, for the maximal growth rate we obtain

$$\frac{\gamma_{r,\max}}{\omega_p} \simeq \frac{v_E}{4c}\sqrt{-\frac{2\omega_p^2}{\omega_\perp\omega_s^4}\frac{k^2c^2}{\frac{\partial}{\partial\omega}\mathcal{D}_\parallel(k,\omega_s)}}. \quad (57)$$

In addition, the resonant instability occurs only for a negative derivative, $\frac{\partial}{\partial\omega}\mathcal{D}_\parallel(k,\omega_s) < 0$, of the longitudinal dispersion function. An analysis shows that there is only one real root $\omega_s = \omega_{r1}^-$ of the equation $\mathcal{D}_\parallel(k,\omega_s) = 0$ which satisfies this condition (see Appendix A for details). This root is negative and is represented here as $\omega_{r1}^-(k) = -\omega_p g(k)$, where the function $g(k)$ is positive and decreases monotonically from $(1+\xi/\gamma_b^3)^{1/2}$ (at $k \simeq 0$) to 1 (at $k \gg k_c$); see Eqs. (A6) and (A1), respectively.

The maximal growth rate (57) is reached at $k = k_{\max}$, which is determined by the resonant condition above,

$\omega_\perp(k) = \omega_0 - \omega_p g(k)$. Assuming short wavelengths ($k \gtrsim k_c$), this equation can be solved iteratively. The result reads as

$$\frac{k_{\max}^2 c^2}{\omega_p^2} \simeq [\tau - g(\kappa)]^2 - \frac{\xi}{\gamma_b} - 1, \tag{58}$$

where $\kappa^2 c^2 = \omega_p^2[\tau(\tau-2) - \xi/\gamma_b]$. Note that the resonant instability occurs only at high frequencies of the RF, $\tau \gtrsim \tau_c \equiv g(\kappa) + (1 + \xi/\gamma_b)^{1/2}$ (for a low-density electron beam this condition is roughly equivalent to $\omega_0 \gtrsim 2\omega_p$).

Substituting Eq. (58) into Eq. (57) we arrive at

$$\frac{\gamma_{r,\max}}{\omega_p} \simeq \frac{v_E}{4c}\sqrt{\frac{[\tau - g(\kappa)]^2 - \xi/\gamma_b - 1}{g(\kappa)[\tau - g(\kappa)]}\frac{1}{1 + \left(\xi/\gamma_b^3\right)H(\kappa)}} \tag{59}$$

with

$$H(\kappa) = \left[\frac{g(\kappa)}{\kappa u_b/\omega_p + g(\kappa)}\right]^3. \tag{60}$$

The maximal growth rate for the resonant instability is strongly simplified for a very low density ($n_b \ll n_e$) or for an ultrarelativistic electron beam ($\gamma_b \gg 1$). In this case the instability occurs at $\tau \gtrsim 2$ and $k_{\max}c = \omega_p[\tau(\tau-2)]^{1/2}$. The growth rate $\gamma_{r,\max}$ is then simply given by

$$\frac{\gamma_{r,\max}}{\omega_p} \simeq \frac{v_E}{4c}\sqrt{\frac{\tau(\tau-2)}{\tau - 1}} \tag{61}$$

and is completely independent on the beam parameters (this is a regime of a purely parametric instability). Note that similar to Eq. (54) for the longitudinal resonant unstable mode the resonant growth rate (61) at $\omega_0 \gg \omega_p$ is scaled as $\gamma_{r,\max} \sim [I_L(\omega_p/\omega_0)]^{1/2}$. Thus, the growth rates of the resonant longitudinal and transversal unstable modes may be of the same order.

In addition to the resonant mode there also exist two nonresonant transversal modes. The dispersion equations for these modes follow from Eq. (41) and are given by $\mathcal{D}_\parallel(k, \omega \pm \omega_0) \simeq 0$, which implies that $\omega = \mp\omega_0 + \omega_s + \Delta\omega_\pm$ (with $|\omega_\pm| \ll |\mp\omega_0 + \omega_s|$). Here $\omega_s = \omega_\parallel^{\rm TS} + i\gamma^{\rm TS}$ [see, e.g., Eqs. (44) and (A4), (A5)] is the solution of the longitudinal dispersion equation in the domain of the two-stream instability which occurs at the low frequencies [$\omega \simeq \omega_\parallel^{\rm TS}(k)$] and at the long wavelengths ($k \leqslant k_c$).

The quantity $\Delta\omega_\pm$ can be roughly estimated using the dispersion equation (41). First, in the leading order, we represent the dispersion function in the form $\mathcal{D}_\parallel(k, \omega \pm \omega_0) \simeq \Delta\omega_\pm \frac{\partial}{\partial\omega}\mathcal{D}_\parallel(k, \omega_s)$. Second, the derivative of the dispersion function is estimated employing Eqs. (A4) and (A5). Assuming a low-density ($n_b \ll n_e$) or an ultrarelativistic ($\gamma_b \gg 1$) electron beam this quantity in the leading order of the dimensionless parameter ξ/γ_b^3 is represented as $\frac{\partial}{\partial\omega}\mathcal{D}_\parallel(k, \omega_s) \simeq (2i/\gamma^{\rm TS})(\omega_p/\omega_\parallel^{\rm TS})^2$. Inserting these results into dispersion equation (41) in the leading order of ξ/γ_b^3, one then finally arrives at

$$\Delta\omega_\pm \simeq -i\frac{k^2 v_E^2}{8}\frac{\omega_p^2 \gamma^{\rm TS}}{(\omega_\parallel^{\rm TS})^2[(\omega_0 \mp \omega_\parallel^{\rm TS})^2 - \omega_\perp^2]}. \tag{62}$$

The real frequencies and the growth rates of the nonresonant modes are simply given by $\omega_r = \mp\omega_0 + \omega_\parallel^{\rm TS}$ and $\gamma = \gamma^{\rm TS} +$ Im$[\Delta\omega_\pm]$, respectively. It should be emphasized that the frequency shift (62) is valid when Im$[\Delta\omega_\pm] \ll \gamma^{\rm TS}$. Moreover, since the nonresonant unstable modes appear in the domain of the two-stream instability with $k \leqslant k_c$, the frequencies $\omega_\parallel^{\rm TS}$ and $\omega_\perp$ in the brackets of the denominator of Eq. (62) can be neglected and, hence, $\Delta\omega_+ \simeq \Delta\omega_-$. The expression (62) can be further simplified recalling that $\omega_\parallel^{\rm TS} \simeq k u_b$ and the ratio $\gamma^{\rm TS}/\omega_\parallel^{\rm TS} \simeq (\xi/\gamma_b^3)^{1/2}$ is almost independent on k [see, e.g., Eqs. (A4) and (A5)]. Therefore, the growth rate of the nonresonant modes is given by

$$\gamma(k) \simeq \gamma^{\rm TS}(k)\left[1 - \frac{1}{8}\left(\frac{v_E}{u_b}\right)^2\left(\frac{\omega_p}{\omega_0}\right)^2\right]. \tag{63}$$

It is noteworthy that this growth rate is proportional to the growth rate $\gamma^{\rm TS}(k)$ of the standard two-stream instability and only the factor in the brackets depends on the laser intensity. Thus, $\gamma(k)$ is weakly sensitive to the laser intensity (because in the present approximation $v_E \ll u_b$ and $\omega_0 > \omega_p$) and is mainly determined by the beam-plasma interaction. In addition, the nonresonant unstable modes do not disappear with decreasing the laser intensity as it occurs for the resonant ones.

V. LONGITUDINAL POLARIZATION OF THE RF ($\mathbf{E_0} \parallel \mathbf{k}$)

With the theoretical formalism presented in Secs. II and III, we now take up another configuration of the laser polarization. In the following we study in detail the parametric two-stream instabilities in the laser-irradiated plasma when the polarization vector of the laser field is parallel to the wave vector $\mathbf{k}$ of the excitations ($\mathbf{E}_0 \parallel \mathbf{k}$), assuming, again, that the beam is directed in the direction of $\mathbf{k}$. It is expected that the beam-plasma and the laser-plasma unstable modes are strongly coupled in this regime compared to the transversal configuration ($\mathbf{E}_0 \perp \mathbf{k}$) since the electrons are effectively driven by a laser radiation in the direction of $\mathbf{k}$ ($\parallel \mathbf{u}_b$) in this case.

Our starting point is the general equation (24) for the harmonics which for the configuration $\mathbf{E}_0 \parallel \mathbf{k} \parallel \mathbf{u}_b$ is decoupled into two independent equations for the longitudinal ($E_\parallel$) and transversal ($\mathbf{E}_\perp$) electric fields, respectively,

$$E_\parallel^{(n)}(0) + \sum_{\ell,s=-\infty}^{\infty} E_\parallel^{(\ell)}(0) J_{\ell-s}(\zeta) J_{n-s}(\zeta)\delta\varepsilon_\parallel(s) = -\delta_{n0} E_\parallel(0)\delta\varepsilon_{b\parallel}(0), \tag{64}$$

$$\mathbf{E}_\perp^{(n)}(0) = \frac{\omega + n\omega_0}{k^2c^2 - (\omega + n\omega_0)^2}\sum_{\ell,s=-\infty}^{\infty}\mathbf{E}_\perp^{(\ell)}(0)\frac{(\omega + s\omega_0)^2}{\omega + \ell\omega_0} \times J_{\ell-s}(\zeta)J_{n-s}(\zeta)\delta\varepsilon_\perp(s) - \delta_{n0}\frac{1}{k^2c^2 - \omega^2}\frac{\omega_b^2}{\gamma_b}\mathbf{E}_\perp(0). \tag{65}$$

Here $\zeta \equiv a(\mathbf{k}\cdot\mathbf{e}) = \pm ka$ and the other notations have been introduced in Secs. II and III. As in the preceding sections we consider throughout an electron plasma neglecting the dynamics of plasma ions.

To exclude the electric field harmonics $E_\parallel^{(n)}$ in Eq. (64), we multiply both sides of this equation by $J_{n-p}(\zeta)J_{\ell-p}(\zeta)$ and

perform a summation over n and p. As a result, we arrive at

$$E_{\parallel}^{(n)}(0) = -E_{\parallel}(0)\delta\varepsilon_{b\parallel}(0)\sum_{s=-\infty}^{\infty}\frac{J_s(\zeta)J_{n+s}(\zeta)}{1+\delta\varepsilon_{\parallel}(-s)}. \quad (66)$$

Thus, the harmonics $E_{\parallel}^{(n)}$ are completely expressed by the total field $E_{\parallel}$. Also, in deriving Eq. (66), we have used the summation formula for the Bessel functions [42]

$$\sum_{s=-\infty}^{\infty} J_{s-\ell}(\zeta)J_{s-n}(\zeta) = \delta_{\ell n}. \quad (67)$$

Next, in Eq. (66), the frequency ω is replaced by $\omega - n\omega_0$ and, using Eq. (23), we perform a summation over n. This yields an equation for the amplitude $E_{\parallel}(0)$ of the electric field

$$[1+\delta\varepsilon_{b\parallel}(0)]E_{\parallel}(0) = \sum_{\ell=-\infty}^{\infty} E_{\parallel}(\ell)\Psi_{\ell}(\zeta)\delta\varepsilon_{b\parallel}(-\ell), \quad (68)$$

where

$$\Psi_{\ell}(\zeta) = \sum_{s=-\infty}^{\infty}\frac{\delta\varepsilon_{\parallel}(-s)}{1+\delta\varepsilon_{\parallel}(-s)}J_{s-\ell}(\zeta)J_s(\zeta). \quad (69)$$

It is noteworthy that in the $\mathbf{E}_0 \parallel \mathbf{k}$ geometry the system of Eqs. (64) and (65) involves all (infinite number) the harmonics of the electric field, whereas, in the transversal case, $\mathbf{E}_0 \perp \mathbf{k}$, considered in Sec. IV each harmonic $E^{(n)}(0)$ with given frequency ω connects only to the nearest neighbors $E^{(n\pm1)}(0)$ and $E^{(n\pm2)}(0)$. These features are the peculiarities of the specific laser polarization directed parallel or perpendicularly to the wave vector $\mathbf{k}$.

Similarly, it is possible to exclude the harmonics $\mathbf{E}_{\perp}^{(n)}$ of the transversal electric field from Eq. (65) and derive an equation for the electric field $\mathbf{E}_{\perp}$,

$$\mathbf{E}_{\perp}(0)\left(k^2c^2+\frac{\omega_b^2}{\gamma_b}-\omega^2\right) = \omega\sum_{\ell,s=-\infty}^{\infty}\mathbf{E}_{\perp}(-\ell)\frac{(\omega+s\omega_0)^2}{\omega+\ell\omega_0} \times J_{\ell-s}(\zeta)J_{-s}(\zeta)\delta\varepsilon_{\perp}(s). \quad (70)$$

First, we note that, at vanishing laser intensity from Eqs. (68)–(70), we recover the standard dispersion equations for the longitudinal, $\mathcal{D}_{\parallel}(k,\omega) = 0$, and transversal, $\mathcal{D}_{\perp}(k,\omega) = 0$, waves given by Eqs. (31) and (37), respectively. Second, within a cold-fluid approximation [the dielectric functions are determined by Eq. (42)] using the summation formula (67) for the transversal modes, we arrive at the same dispersion relation as in Eq. (43). Therefore, within this approximation the laser field has no influence on the dispersion properties of the transversal modes, which are stable in this case. Third, in contrast to the longitudinal modes (68), the transversal ones are only weakly sensitive to the beam parameters [see the left-hand side of Eq. (70)] and the instability of these modes is parametric in nature. These instabilities have been studied previously in Ref. [44]. Consequently, in the following we consider throughout only the dynamics of the longitudinal modes $E_{\parallel}$.

As was mentioned in the previous sections, the dispersion equation of the perturbations can be deduced, in principle, from Eq. (68) by solving this system of equations by iteration to any order of accuracy. However, to gain more insight we consider the long-wavelength limit of Eq. (68) when the parameter $|\zeta| = ka$ is small, which suffices to restrict the analysis of the system (68) to the harmonics $E_{\parallel}(0)$ and $E_{\parallel}(\pm1)$. In this case, we obtain the following dispersion equations for the longitudinal modes:

$$\mathcal{D}_{\parallel}(k,\omega) = \frac{k^2a^2}{4}\delta\varepsilon_{b\parallel}(k,\omega)[P_1(k,\omega)+P_{-1}(k,\omega)], \quad (71)$$

where

$$P_{\pm1}(k,\omega) = \frac{\delta\varepsilon_{b\parallel}(k,\omega\pm\omega_0)+\varepsilon_{\parallel}(k,\omega)}{\mathcal{D}_{\parallel}(k,\omega\pm\omega_0)}\left[\frac{\varepsilon_{\parallel}(k,\omega\pm\omega_0)}{\varepsilon_{\parallel}(k,\omega)}-1\right]. \quad (72)$$

The dispersion equation (71) can be compared with Eqs. (40) and (41) obtained for the $\mathbf{E}_0 \perp \mathbf{k}$ geometry. It should be emphasized that, unlike the $\mathbf{E}_0 \perp \mathbf{k}$ geometry, the dispersion equation (71) [see also the more correct relation (68)] in the absence of the charged-particle beam ($\delta\varepsilon_{b\parallel} = 0$) yields the standard dispersion equation $\varepsilon_{\parallel}(k,\omega) = 0$ for the longitudinal modes. Thus, in this case, the laser radiation with $\mathbf{E}_0 \parallel \mathbf{k}$ does not influence the dispersion properties of the plasma in the $\mathbf{k}$ direction but it affects the dispersion relation in the transversal direction [see Eq. (70)]. This result sounds paradoxical, considering that the plasma oscillations should be effectively driven by the laser field in the $\mathbf{E}_0 \parallel \mathbf{k}$ configuration. However, let us recall that the dynamics of the plasma ions is completely neglected here. In reality, the laser radiation with $\mathbf{E}_0 \parallel \mathbf{k}$ stimulates low-frequency (typically with the ion plasma frequency) electron-ion-coupled oscillations [37,38] and the dispersion relation is not simply given by the equation $\varepsilon_{\parallel}(k,\omega) = 0$.

The simplest way to investigate the parametric TS instabilities determined by Eq. (71) is the cold-fluid model when the dielectric functions are given by Eq. (42). In this specific case, the function $\Psi_{\ell}(\zeta)$ is evaluated analytically in Appendix B [Eqs. (B3) and (B4)] using the Newberger's summation formula [46]. Since the function $\Psi_{\ell}(\zeta)$ decays exponentially with ℓ the harmonics $E_{\parallel}(\ell)$ in Eq. (68) and the corresponding dispersion relations can be effectively evaluated numerically to any order of ℓ. Furthermore, within the cold-fluid approximation, it is possible to derive a dynamical equation for the complex amplitude of the excited waves. This is done in Appendix C; see Eq. (C6).

One characteristic feature of the dispersion equation (71) for the longitudinal modes in $\mathbf{E}_0 \parallel \mathbf{k}$ geometry is the absence of the contribution of the transverse modes. We consider, first, the situation (i) (see Sec. IV A) which corresponds to the low-frequency [$\omega \sim \omega_{\parallel}^{\mathrm{TS}}(k)$], long-wavelength excitations. Close to the Čherenkov resonance, $\omega \simeq ku_b$, we look for the solution of the dispersion equation (71) in the form $\omega = ku_b + \omega_1$, where $|\omega_1| \ll ku_b$. In this case, the instability occurs at $ku_b \lesssim \omega_p$ with the growth rate ($\omega_1 = i\gamma$) [cf. with Eqs. (44) and (46)]

$$\frac{\gamma(k)}{\omega_p} = \left(\frac{\xi}{\gamma_b^3}\right)^{1/2}\frac{ku_b}{\sqrt{\omega_p^2-(ku_b)^2}}G(k,ku_b), \quad (73)$$

where

$$G(k,\omega) = \left\{1-\frac{k^2a^2}{4}[P_1(k,\omega)+P_{-1}(k,\omega)]\right\}^{1/2}. \quad (74)$$

Note that Eq. (73) is valid far from the roots of the equation $\varepsilon(\omega \pm \omega_0) = \omega_b^2/\gamma_b^3\omega_0^2$, where $\varepsilon(\omega) = 1 + \delta\varepsilon(\omega)$ is the dielectric function in a cold-fluid approximation.

The maximal growth rate is achieved at $ku_b \simeq \omega_p$. Similarly to Eq. (46), the relation (73) is clearly invalid in this case and more rigorous treatment of the dispersion equation for the frequency correction ω_1 yields a fourth-order algebraic equation

$$\omega_1^4 = \frac{\xi\omega_p^3}{2\gamma_b^3}\left[\omega_1 + \frac{v_E^2}{8u_b^2}\frac{\omega_p\xi}{\gamma_b^3\tau^4}(p_1 + p_{-1})\right]. \tag{75}$$

Here

$$p_{\pm1} = \frac{\varepsilon(\omega_0 \pm \omega_p)}{\varepsilon(\omega_0 \pm \omega_p) - \omega_b^2/\gamma_b^3\omega_0^2}, \tag{76}$$

and the laser frequency ω_0 is not too close to the value $2\omega_p[1 + (\xi/2\gamma_b^3)]$. It can be shown that the second term in the right-hand side of Eq. (75) is systematically smaller than the first one. Neglecting this term, we arrive at the maximal growth rate $\gamma_{\max}^{\mathrm{TS}}$ of the two-stream instability; see Eq. (45). Thus, as expected, in the situation (i) the maximal growth rate is only weakly affected by the RF.

Next we consider a high-frequency $[\omega > \omega_{\parallel}^{\mathrm{TS}}(k)]$, short-wavelength regime with $ku_b \gtrsim \omega_c$. The nonresonant coupling similar to (iii) is determined by the intersection of the different roots of the dispersion equations $\mathcal{D}_{\parallel}(k,\omega \pm \omega_0) \simeq 0$. If ω_{s1} and ω_{s2} are two different roots of the parallel dispersion function, $\mathcal{D}_{\parallel}(k,\omega_{s1}) = \mathcal{D}_{\parallel}(k,\omega_{s2}) = 0$, the above-mentioned intersection of the roots simply yields $\omega_{s1} = \omega_{s2} + 2\omega_0$. This equation implies that both roots ω_{s1} and ω_{s2} should be real, which is possible only outside the domain of the two-stream instability ($ku_b \gtrsim \omega_c$; see also Appendix A). In addition, the frequency shift $\Delta\omega$ determined by the relation $\omega + \omega_0 = \omega_{s1} + \Delta\omega$ (or, alternatively, $\omega - \omega_0 = \omega_{s2} + \Delta\omega$), is also real and can be calculated from the dispersion equation (71). Therefore, in this case, the nonresonant coupling merely shifts the real frequencies of the modes and does not cause any instability in the beam-plasma system.

Instability may occur in situation (ii) with the resonant coupling. In this case, $\mathcal{D}_{\parallel}(k,\omega) \simeq 0$ and $\mathcal{D}_{\parallel}(k,\omega \pm \omega_0) \simeq 0$. Again introducing two different real roots ω_{s1} and ω_{s2} of the parallel dispersion function, we consider the frequency shift $\Delta\omega$ with $\omega = \omega_{s2} + \Delta\omega$, such that $|\Delta\omega| \ll |\omega_{s1,2}|$. The resonant coupling occurs when $\omega_{s2} = \omega_{s1} \pm \omega_0$. Substituting this relation and the frequency ω into dispersion equation (71) and taking into account the smallness of the quantity $\Delta\omega$, we obtain

$$\Delta\omega^2 \simeq \frac{k^2a^2}{4}\frac{[\varepsilon(\omega_{s2}) - \varepsilon(\omega_{s1})]^2}{\frac{\partial}{\partial\omega}\mathcal{D}_{\parallel}(k,\omega_{s1})\frac{\partial}{\partial\omega}\mathcal{D}_{\parallel}(k,\omega_{s2})}. \tag{77}$$

It is seen that this expression is symmetric with respect to the exchange of the roots ω_{s1} and ω_{s2} and yields an unstable mode if the derivatives of the longitudinal dispersion functions in the denominator of Eq. (77) have different signs. The resonant coupling condition, $\omega_{s2} = \omega_{s1} \pm \omega_0$, and the restriction on the signs of the derivatives of the longitudinal dispersion functions in Eq. (77) reduce the possible candidates for the quantities ω_{s1} and ω_{s2}. From Appendix A it follows that there are only three choices as follows: (a) $\omega_{s1}(k) = \omega_{r1}^-(k)$ and $\omega_{s2}(k) = \omega_{r3}(k)$ with $\omega_{r3}(k) = \omega_0 + \omega_{r1}^-(k)$; (b) $\omega_{s1}(k) = \omega_{r1}^+(k)$ and $\omega_{s2}(k) = \omega_{r2}(k)$ with $\omega_{r2}(k) = \omega_0 + \omega_{r1}^+(k)$; and (c) $\omega_{s1}(k) = \omega_{r1}^+(k)$ and $\omega_{s2}(k) = \omega_{r1}^-(k)$ with $\omega_{r1}^+(k) = \omega_0 + \omega_{r1}^-(k)$. In these cases, the derivatives in the denominator of Eq. (77) have different signs and the corresponding modes are unstable. The positions $k_{\max}$ of the maximal growth rates of these modes can be determined from the resonant coupling condition. Using the asymptotic behavior of the roots $\omega_{r1}^{\pm}(k)$, $\omega_{r2}(k)$, and $\omega_{r3}(k)$ at $k \geqslant k_c$, Eqs. (A1)–(A3), respectively, we introduce four new functions $f_{\pm}(k)$ and $h_{\pm}(k)$, which are determined through relations

$$\begin{pmatrix}\omega_{r2}(k)\\ \omega_{r3}(k)\end{pmatrix} = ku_b \mp \omega_p\frac{\sqrt{\xi}}{\gamma_b^{3/2}}h_{\pm}(k), \tag{78}$$

$$\omega_{r1}^{\pm}(k) = \pm\omega_p\left[1 + \frac{\xi}{\gamma_b^3}f_{\pm}(k)\right]. \tag{79}$$

Then, in the cases (a) and (b) with $\omega_{s2} = \omega_{s1} + \omega_0$, the resonant coupling conditions for the determination of $k_{\max}$ in a leading order of the parameter ξ/γ_b^3 yields a pair of the transcendental equations

$$ku_b = \omega_0 \pm \omega_p \pm \frac{\sqrt{\xi}}{\gamma_b^{3/2}}\omega_p h_{\pm}(k), \tag{80}$$

which can be solved iteratively. Here the minus and plus signs are related to the cases (a) and (b), respectively. Since the functions $h_{\pm}(k)$ at $k \geqslant k_c$ behave as $h_{\pm}(k) = 1 + \mathrm{O}[(\omega_p/ku_b)^2]$ (see Appendix A) within zero order, the last term in Eq. (80) can be neglected, which yields $\kappa_{\pm} = (\omega_0 \pm \omega_p)/u_b$. Substituting this value into the arguments of the functions $h_{\pm}(k)$ in the last term of Eq. (80), one obtains the corrections to $\kappa_{\pm}$. The maximal growth rates are obtained from Eq. (77), where $k = k_{\max}$. In the leading order of ξ/γ_b^3 the result reads

$$\frac{\gamma_{r,\max}^{\pm}}{\omega_p} \simeq \frac{v_E}{4u_b}\left(\frac{\xi}{\gamma_b^3}\right)^{1/4}\left|\frac{\tau \pm 2}{\tau \pm 1}\right|[h_{\pm}(\kappa_{\pm})]^{3/2}. \tag{81}$$

For an estimate the approximate expressions $h_{\pm}(\kappa_{\pm}) \simeq 1 + (1/2)(\tau \pm 1)^{-2}$ for the functions $h_{\pm}(k)$ can be used. Here $\gamma_{r,\max}^-$ and $\gamma_{r,\max}^+$ are related to the maximal growth rates in the regimes (a) and (b), respectively. Let us note that for a validity of Eq. (81) in the regime (a) the laser frequency ω_0 should not be too close to the plasma frequency. From Eqs. (71) and (77) it is straightforward to obtain the profiles of the resonant growth rates in the regimes (a) and (b). Introducing the frequency mismatch $\delta = \omega_{s2} - \omega_{s1} - \omega_0$, these profiles are determined by

$$\gamma_r^{\pm}(k) = \tfrac{1}{2}\sqrt{4(\gamma_{r,\max}^{\pm})^2 - \delta^2(k)}. \tag{82}$$

Here $\gamma_{r,\max}^{\pm}$ are the maximal growth rates [see Eq. (81)] which are achieved at $\delta = 0$. It is seen that the quantities $\gamma_r^-(k)$ and $\gamma_r^+(k)$ vanish at $k_{1;2} \simeq \kappa_- \pm 2\gamma_{r,\max}^-/u_b$ and $k_{3;4} \simeq \kappa_+ \pm 2\gamma_{r,\max}^+/u_b$, respectively.

Consider now the regime (c) when $\omega_{s2} = \omega_{s1} - \omega_0$. In this case, the resonant coupling condition reads

$$\omega_0 - 2\omega_p = \omega_p\frac{\xi}{\gamma_b^3}[f_+(k) + f_-(k)]. \tag{83}$$

It is clear that this relation can be satisfied only at $\omega_0 > 2\omega_p$ since the functions $f_{\pm}(k)$ are positive (see Appendix A). On

the other hand, ω_0 should be sufficiently close to $2\omega_p$ because the dimensionless parameter ξ/γ_b^3 is small. Assuming, for instance, $\tau - 2 \ll \xi/\gamma_b^3$ and employing the results of the Appendix A the solution of Eq. (83) reads as $k_0 u_b/\omega_p \simeq (\xi/\gamma_b^3)^{1/2}(\tau-2)^{-1/2} \gg 1$. This value of k determines the position of the maximal growth rate in (c) which is obtained from Eq. (77) and is given by

$$\frac{\gamma_{r,\max}}{\omega_p} \simeq \frac{v_E}{u_b}\frac{\tau-2}{\tau} \ll \frac{v_E}{u_b}\frac{\xi}{\tau\gamma_b^3}. \tag{84}$$

Confronting this relation with the growth rates $\gamma^{\pm}_{r,\max}$, we conclude that $\gamma_{r,\max} \ll \gamma^{\pm}_{r,\max}$. In addition, it should be noted that, in general, $k_0 \gg \kappa_{\pm}$ and the growth rate $\gamma_{r,\max}$ may be strongly shifted toward very large k values.

Unlike $\mathbf{E}_0 \perp \mathbf{k}$ geometry the beam-plasma and the laser-plasma parametric modes are strongly coupled here. As a result, the resonant modes (81) and (84) depend essentially on the laser intensity and the beam density.

Let us now compare the growth rates in the regimes (a) and (b) for the resonant unstable modes with the quantity $\gamma^{\mathrm{TS}}_{\max}$, assuming, for simplicity, $\tau \gg 1$ ($\omega_0 \gg \omega_p$). In this case, $\gamma^{+}_{r,\max} \simeq \gamma^{-}_{r,\max}$. It is seen that $\gamma^{\pm}_{r,\max}$ exceed the growth rate $\gamma^{\mathrm{TS}}_{\max}$ of the two-stream instability at sufficiently intense RF, $v_E/c > 3.02(\gamma^{\mathrm{TS}}_{\max}/\omega_p)^{1/4}$. It is clear that this condition requires very low density beams (compared to n_e) and is increasingly difficult to fulfill with increasing n_b. Also, the growth rates in Eq. (81) should be compared with the growth rates of the resonant longitudinal Eq. (54) and the transversal Eqs. (59) and (61) modes as well as with the nonresonant longitudinal modes Eqs. (55) and (56) excited in $\mathbf{E}_0 \perp \mathbf{k}$ geometry. Again assuming, for simplicity, the $\omega_0 \gg \omega_p$ limit, we conclude that the unstable modes grow much faster in this geometry, where the parametric effects are more pronounced. However, it should be emphasized that the resonant unstable modes in $\mathbf{E}_0 \perp \mathbf{k}$ geometry are only effectively excited starting with the threshold frequency $\omega_0 \simeq 2\omega_p$ of the laser radiation. Below this threshold (with $\omega_0 \lesssim 2\omega_p$), only the unstable mode (63) in the long-wavelength domain and the modes (55), (56), and (81) in the short-wavelength domain are excited in $\mathbf{E}_0 \perp \mathbf{k}$ and $\mathbf{E}_0 \parallel \mathbf{k}$ configurations, respectively.

VI. NUMERICAL TREATMENT

Using the theoretical findings of Secs. III–V, we present here the results of our numerical calculations of the growth rates for the longitudinal and the transversal unstable modes assuming the transverse ($\mathbf{E}_0 \perp \mathbf{k}$) and the parallel ($\mathbf{E}_0 \parallel \mathbf{k}$) configuration of the RF amplitude $\mathbf{E}_0$ with respect to the wave vector $\mathbf{k}$. The calculations have been done for an electron beam with a small dimensionless density parameters $\xi = (\omega_b/\omega_p)^2 = n_b/n_e = 0.1$ and $\xi = 0.3$ and for a relativistic factor $\gamma_b = 5$. For the laser intensity parameter $\alpha = v_E^2/c^2$ we have adopted the values $\alpha = 0, 0.01, 0.1$, and 0.2. It is convenient to represent the laser intensity parameter in the form $\alpha = (I_L/I_0)\lambda_0^2$, where $I_0 = 1.37 \times 10^{18}$ W μm^2/cm^2 and the wavelength (λ_0) and the intensity (I_L) of the laser field are measured in units μm and W/cm^2, respectively. The laser frequency is measured in the units of the plasma frequency, $\tau = \omega_0/\omega_p > 1$. In our numerical calculations, this parameter varies in a wide interval, $1.2 \leqslant \tau \leqslant 4$. Throughout in this section the growth rates are measured in units of plasma frequency ω_p and are calculated as a function of ku_b/ω_p for several laser intensities and frequencies. Note that the chosen parameters both for electron beam and RF are typical for FIS for inertial confinement fusion [7]. Assuming, for instance, radiation field with $\lambda_0 = 0.5$ μm, the parameter $\alpha = 0.2$ corresponds to the intensity $I_L \simeq 10^{18}$ W/cm^2 of the RF.

First, we consider the transverse geometry with $\mathbf{E}_0 \perp \mathbf{k}$. In this case, the basic properties of the dispersion relations for the beam-plasma system have been studied in Sec. IV. In general, we have found that the simplified treatments of Secs. IV and V agree qualitatively well with the exact numerical solutions. However, it is clear that these simplified treatments are not capable to resolve all details and the branches of the spectrum of the unstable modes in the ω-k plane.

Within $\mathbf{E}_0 \perp \mathbf{k}$ geometry we now consider the case of the longitudinal unstable modes ($\gamma = \gamma_{\parallel}$) when the dispersion relations are determined by Eq. (40). As mentioned in Sec. IV A this is a regime when the purely two-stream and the parametric modes are only weakly coupled and their spectra are well separated in the ω-k plane. Therefore, the different modes (beam-plasma or parametric) are only weakly sensitive either to the electron beam parameters or the intensity of the RF. From Eq. (40) it is seen [see also the simplified version of this relation, Eq. (51)] that in a cold-fluid approximation there are 10 solutions of this equation, but only some of them correspond to the unstable modes with $\gamma > 0$. In addition, these unstable modes are excited with different real frequencies. To demonstrate this feature in Fig. 1, the growth rates are shown for the laser frequency $\omega_0 = 1.2\omega_p$. In this case, we have found numerically that there are only three solutions which correspond to the unstable modes, and, as an example, two solutions are shown in the left and right panels of Fig. 1. The different curves correspond to the laser dimensionless intensities $\alpha = 0.01$ (dashed lines), $\alpha = 0.1$ (dotted lines), and $\alpha = 0.2$ (dash-dotted lines). The solid lines with $\alpha = 0$ represent the growth rate of the standard two-stream instability, Eq. (44). Two panels of Fig. 1 correspond to the modes with different real frequencies ω_r. We denote tentatively the solutions with different ω_r as branches I, II, III, and so on. In the left panel of Fig. 1 up to the value $k_2 c/\omega_p = (\tau^2-1)^{1/2} \simeq 0.6$ ($k = k_2$ corresponds to the vanishing frequency mismatch, $\delta = 0$, introduced in Sec. IV A), the real frequency is $\omega_r = 0$ (branch I), while at $k_2 \leqslant k \leqslant k_1$ it is given by $\omega_r = \omega_g(k)$ (branch II). In Fig. 1 the growth rates sharply tend to zero at $k = k_1$. [For the approximate definition of the quantity k_1, see the paragraph above Eq. (56)]. The spectrum $\omega_g(k)$ corresponds to the real frequency of the nonresonant longitudinal modes derived approximately in Sec. IV A for the negative frequency mismatch ($\delta < 0$). In the approximate form it is given by Eq. (56), where, however, the minus sign has to be replaced by the plus sign. In the approximate treatment of Sec. IV A, Eqs. (55) and (56) correspond to branches I and II, respectively. Thus, the boundary between branches I and II is determined by $\delta = 0$ (or $k = k_2$). In branch I the growth rate at $k \lesssim k_2$ increases almost linearly with k, $\gamma(k) \simeq k v_E[2(\tau^2-1)]^{-1/2}$, in agreement with Eq. (55). Finally, in Fig. 1 (right panel), the real frequencies of the modes at $0 \leqslant k \leqslant k_c$ and $k_c \leqslant k \leqslant \max[k_c; k_1]$ coincide with the real frequency of the standard

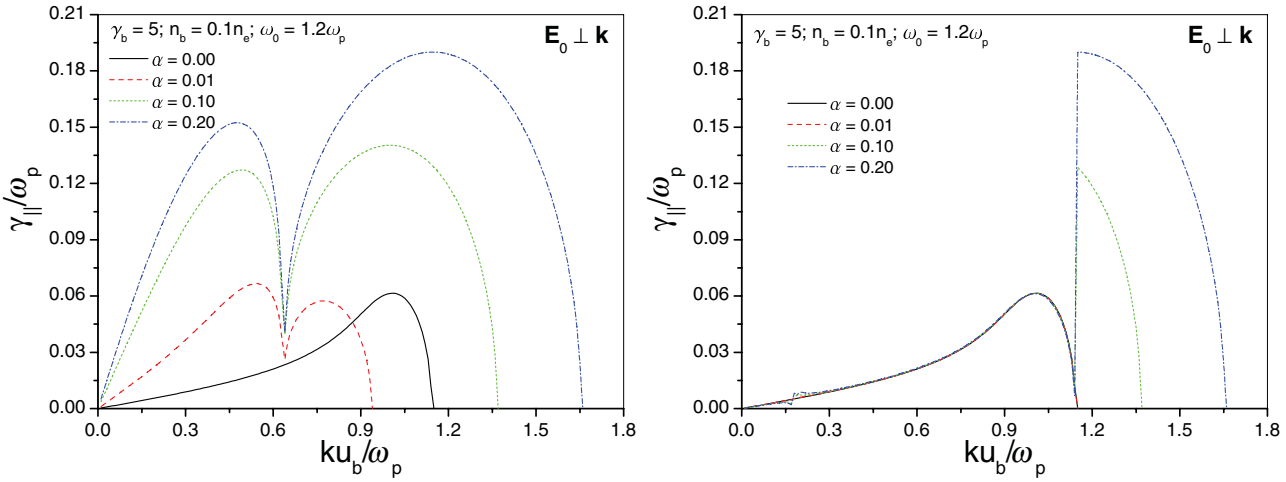

FIG. 1. (Color online) The growth rate $\gamma_\parallel$ (in units of plasma frequency ω_p) of the longitudinal unstable modes in terms of ku_b/ω_p obtained by numerical solution of the dispersion equation (40) in $\mathbf{E}_0 \perp \mathbf{k}$ configuration for $\gamma_b = 5, n_b = 0.1n_e, \omega_0 = 1.2\omega_p, \alpha = 0$ (solid line), $\alpha = 0.01$ (dashed line), $\alpha = 0.1$ (dotted line), and $\alpha = 0.2$ (dash-dotted line). The left and the right panels correspond to branches I, II and III, IV, respectively, introduced in the text.

two-stream instability, $\omega_r = \omega_\parallel^{\mathrm{TS}}(k)$ [branch III; see Eq. (44)] and $\omega_r = \omega_0 + \omega_\perp(k)$ (branch IV), respectively. Here $\omega_\perp(k)$ is given by Eq. (43). Let us note that the boundary $k = k_2$ between I and II does not depend on the intensity of the RF while the upper boundary $k = k_1$ of branches II and IV (at $k_1 > k_c$) is shifted toward shorter wavelengths roughly as $k_1 \simeq k_2[1 + \mathrm{O}(\alpha^{1/3})]$ with increasing laser intensity. It is clear that at a smaller intensity of the RF when $k_1 < k_c$, branch IV disappears. As a general rule, we observe that at $k_c \leqslant k \leqslant k_1$ the growth rates in branch IV are part of branch II, except in the case of the low-intensity RF with $k_1 < k_c$ (cf. the dashed curves in Fig. 1 with $\alpha = 0.01$). In this low-intensity limit, branch IV disappears while branch III is nearly the same as the standard branch for the two-stream instability (solid curves in Fig. 1). Thus, at $\omega_0 \gtrsim \omega_p$ and at small intensities of the RF ($k_1 < k_c$), the parametric two-stream instability occurs in branch III with the growth rate $\simeq \gamma^{\mathrm{TS}}(k)$, which is only weakly affected by the RF. At higher intensities of the RF (with $k_1 > k_c$) a new unstable branch IV is formed. Branches I, II, and IV are formed due to the parametric excitations and are almost insensitive to the electron beam.

Next, in Fig. 2, the longitudinal growth rates are shown for the higher laser frequencies $\omega_0 = 2\omega_p$ (left panel) and $\omega_0 = 4\omega_p$ (right panel). As expected, the different branches shown in Fig. 1 are mixed with increasing ω_0 and, in addition, more and more new branches for the unstable modes are formed. As an example, in Fig. 2, only two solutions of the dispersion equation (40) are shown which involve the basic features of branches I, II, III, and IV introduced above. Note that in these particular examples with higher laser frequencies, $k_2 \simeq \omega_0/c$ exceeds the upper boundary k_c of the two-stream instability, and, therefore, $k_1 > k_c$ for an arbitrary intensity of the RF. As has been pointed out above, the approximate growth rates given by Eqs. (55) and (56) are not capable in these regimes to resolve all specific branches shown in Fig. 2. The most important feature shown in Fig. 2 is that

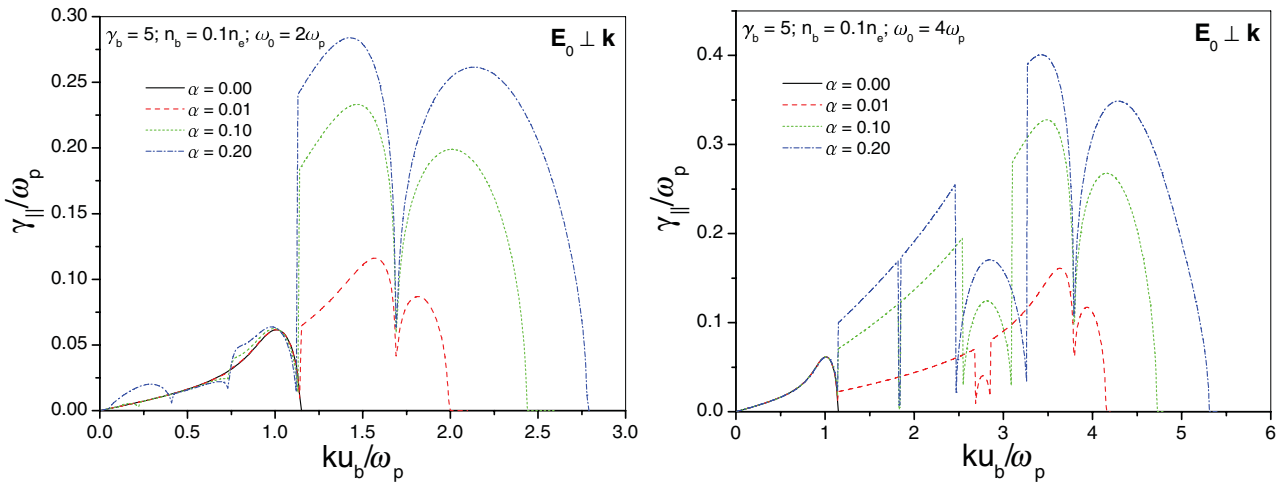

FIG. 2. (Color online) Same as in Fig. 1 but for the higher laser frequencies $\omega_0 = 2\omega_p$ (left panel) and $\omega_0 = 4\omega_p$ (right panel). Note the different scales in the left and the right panels.

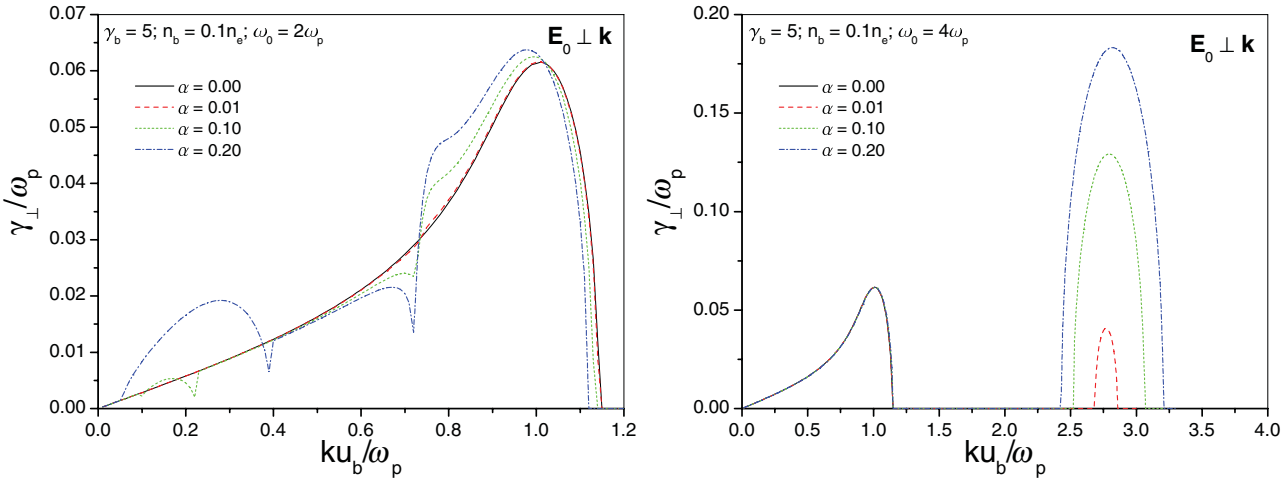

FIG. 3. (Color online) The growth rate $\gamma_\perp$ (in units of plasma frequency ω_p) of the transversal unstable modes in terms of ku_b/ω_p obtained by numerical solution of the dispersion equation (41) in the $\mathbf{E}_0 \perp \mathbf{k}$ configuration for $\gamma_b = 5$, $n_b = 0.1n_e$, $\omega_0 = 2\omega_p$ (left panel), $\omega_0 = 4\omega_p$ (right panel), and for $\alpha = 0$ (solid line), $\alpha = 0.01$ (dashed line), $\alpha = 0.1$ (dotted line), and $\alpha = 0.2$ (dash-dotted line). Note the different scales in the left and the right panels.

the domain of the instability in the k space is broadened and accompanied by an increase of the maximal growth rate with increasing ω_0. It is also noteworthy that the formation of the resonant growth rate in the spectrum of the unstable modes at $\omega_0 \gtrsim 2\omega_p$ derived approximately in Sec. IV A; see Eqs. (52)–(54). Let us recall that the resonant unstable mode is not excited at $\omega_0 < 2\omega_p$ (see Sec. IV A) and, hence, this mode is not visible on Fig. 1. As predicted by Eqs. (52)–(54), the resonant coupling at $\omega_0 = 2\omega_p$ (Fig. 2, left panel) is only weakly pronounced with the maximal growth rate $\gamma_{r,\max}/\omega_p \simeq \alpha/6$ and $k_{r,\max} \simeq (\omega_p/c)(\alpha/3)^{1/2}$ while at higher frequency $\omega_0 = 4\omega_p$ (Fig. 2, right panel) it is strongly increased and is shifted toward the short wavelengths, $\gamma_{r,\max}/\omega_p \sim (\alpha\tau/4)^{1/2}$ with $k_{r,\max} \sim \omega_0/c$. In Fig. 2 (right panel), the resonant growth rate is determined by the curve with the maximum located around $ku_b/\omega_p \sim 3$.

The growth rates for the transversal unstable modes are demonstrated in Fig. 3 for the $\mathbf{E}_0 \perp \mathbf{k}$ geometry and for $\omega_0 = 2\omega_p$ (left panel) and $\omega_0 = 4\omega_p$ (right panel). These growth rates are obtained by the numerical solution of the dispersion equation (41) for the transversal modes. The results for the smaller laser frequencies (with $\omega_0 < 2\omega_p$) are not shown in Fig. 3. This is because only the nonresonant modes with the growth rates approximately given by Eqs. (62) and (63) are possible in this case, as discussed in Sec. IV B. We have found numerically that in this frequency regime the growth rate only weakly deviates from the growth rate $\gamma^{\mathrm{TS}}(k)$ [see Eq. (44)] of the standard two-stream instability which is supported by the approximate Eq. (63). Thus, in Fig. 3, the nearly resonant and the resonant cases are shown with $\omega_0 = 2\omega_p$ and $\omega_0 = 4\omega_p$, respectively. In the first case, the high-frequency ($\omega \simeq \omega_0 - \omega_p$, see Sec. IV B) resonant mode is not yet formed but it may interfere with the two-stream mode, essentially changing the growth rate; see Fig. 3 (left panel). This effect increases with the laser intensity. In the second case, the resonant mode is well separated from the two-stream mode and forms (see Fig. 3, right panel) an isolated maximum at $k_{\max}$ determined approximately by Eq. (58) (or, roughly, $k_{\max} \simeq (\omega_p/c)[\tau(\tau-1)]^{1/2}$). The maximal growth rate of the resonant mode is well described by Eq. (59). It is seen that the position of the maximum is almost independent from the laser intensity while the maximum growth rate increases as $\sim\alpha^{1/2}$ with the parameter α. The dependence of the growth rate $\gamma_\perp(k)$ of the resonant mode on the frequency ω_0 of the laser field for fixed plasma density and RF intensity is also noteworthy. The maximal growth rate $\gamma_{r,\max}$ increases with ω_0 and is shifted toward larger k, achieving the maximal value at $\omega_0 \simeq 3.4\omega_p$. For larger frequencies, the maximal growth rate is scaled as $\gamma_{r,\max} \sim [I_L(\omega_p/\omega_0)]^{1/2}$ and falls with ω_0.

Finally, in Figs. 4 and 5, the growth rate $\gamma_\parallel$ of the longitudinal unstable modes excited in the case $\mathbf{E}_0 \parallel \mathbf{k}$ are shown. These results have been obtained by numerical solution of the dispersion equation (71) with Eq. (72) for $\omega_0 = 1.2\omega_p$, $\omega_0 = 2\omega_p$ (Fig. 4), and $\omega_0 = 4\omega_p$ (Fig. 5). As mentioned in Sec. V, the coupling between the parametric and the two-stream modes may be very effective in this configuration, which is supported by the analytical results obtained in Sec. V. The growth rate (84) of the resonant unstable mode in regime (c) is much smaller than $\gamma^{\pm}_{r,\max}$ and is not shown here. In both panels of Fig. 4 the frequency of the RF is rather small and, hence, only the right-side resonant mode with $\gamma^{+}_{r,\max}$ is excited at $\kappa_+ u_b \simeq \omega_0 + \omega_p$ [see Eq. (81)]. The left-side resonant mode with $\gamma^{-}_{r,\max}$ is formed at $\kappa_- u_b \simeq \omega_0 - \omega_p$ and in Fig. 4 it is merged with the two-stream mode and is not distinguishable. To gain more insight in Fig. 5 we demonstrate the growth rates for the larger laser frequency $\omega_0 = 4\omega_p$, assuming that $n_b = 0.1n_e$ (left panel) and $n_b = 0.3n_e$ (right panel). Now, with increasing laser frequency ω_0, the left-side resonant mode is clearly visible in Fig. 5 and the corresponding growth rate $\gamma^{-}_{r,\max}$ is smaller than $\gamma^{+}_{r,\max}$, as predicted by Eq. (81). The domains where the growth rates of the left-side and the right-side resonant modes are nonzero can be approximated as $\Delta k_\pm \simeq 4\gamma^{\pm}_{r,\max}/u_b$; see Eq. (82). Furthermore, both $\gamma^{\pm}_{r,\max}$ and $\Delta k_\pm$ increase with electron density, as shown in Fig. 5

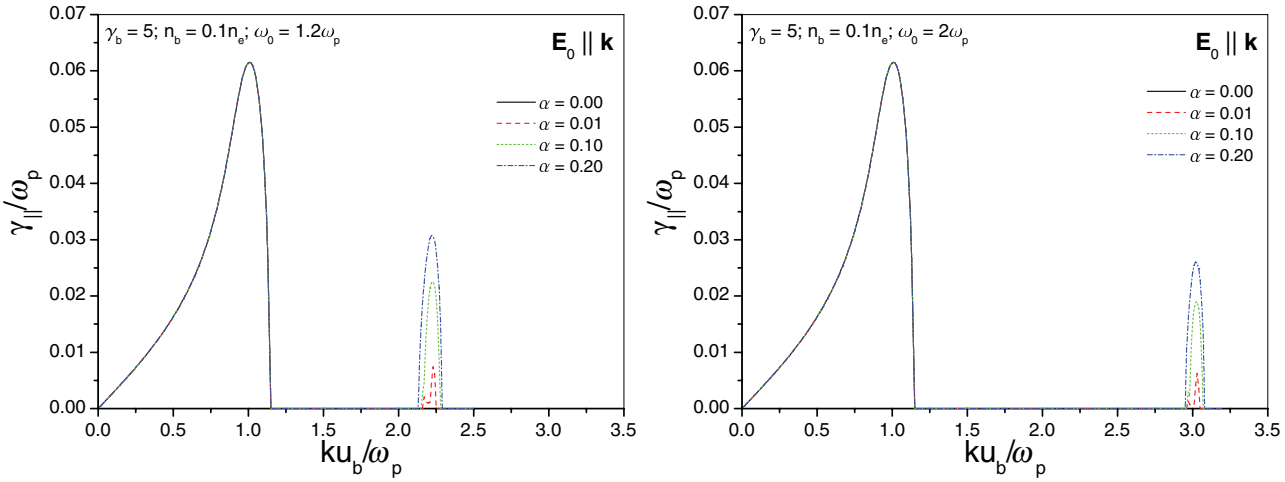

FIG. 4. (Color online) The growth rate $\gamma_\parallel$ (in units of plasma frequency ω_p) of the longitudinal unstable modes in terms of ku_b/ω_p obtained by numerical solution of the dispersion equation (71) with Eq. (72) in $\mathbf{E}_0 \parallel \mathbf{k}$ configuration for $\gamma_b = 5$, $n_b = 0.1n_e$, $\omega_0 = 1.2\omega_p$ (left panel), $\omega_0 = 2\omega_p$ (right panel), and for $\alpha = 0$ (solid line), $\alpha = 0.01$ (dashed line), $\alpha = 0.1$ (dotted line), and $\alpha = 0.2$ (dash-dotted line).

(right panel). Note that the growth rates $\gamma^{\rm TS}_{\rm max}$ and $\gamma^{\pm}_{r,\,\rm max}$ increase approximately as $\sim n_b^{1/3}$ and $\sim n_b^{1/4}$ with the beam density n_b, respectively. In the parameter regimes shown in Figs. 4 and 5 the electron beam is somewhat dense and the condition $\gamma^{\pm}_{r,\,\rm max} > \gamma^{\rm TS}_{\rm max}$ requires relativistic intensities for the RF (with $v_E > c$) which cannot be fulfilled in the present approximation.

In the numerical examples shown in Figs. 1–5 the parametric instabilities are comparable or even stronger than the standard two-stream instability. The stronger effect is expected rather in the case of the transversal polarization $\mathbf{E}_0 \perp \mathbf{k}$ of the laser field both for the longitudinal and transversal modes. In addition, the k domain of the parametric instability is comparable or even larger than the range k_c of the standard two-stream instability. Although an effective coupling between laser-plasma and beam-plasma modes is expected in the case of the parallel polarization of the laser field, $\mathbf{E}_0 \parallel \mathbf{k}$, the resulting growth rates and their k domains are, in general, essentially smaller than those obtained for the transversal polarization. This is not surprising because the effects of the laser radiation and the REB on the dispersion properties of plasma are treated here perturbatively when the coupling between both effects is rather weak.

VII. SUMMARY AND CONCLUDING REMARKS

In this paper, we have presented a theoretical study of the growth rates of the unstable modes excited simultaneously by a laser field and a relativistic beam of charged particles moving in an isotropic plasma. The laser field is treated in the long-wavelength limit (dipole approximation) and the plasma particles are considered nonrelativistic. In addition, an ultrarelativistic beam of the charged particles is considered and the influence of the laser field on the beam is neglected. The dynamics of the beam-plasma system in the presence of the RF is studied by the linearized relativistic and nonrelativistic Vlasov kinetic equations for the distribution functions of the beam and the plasma, respectively, as well as by the linearized Maxwell equations for the electromagnetic fields. The full

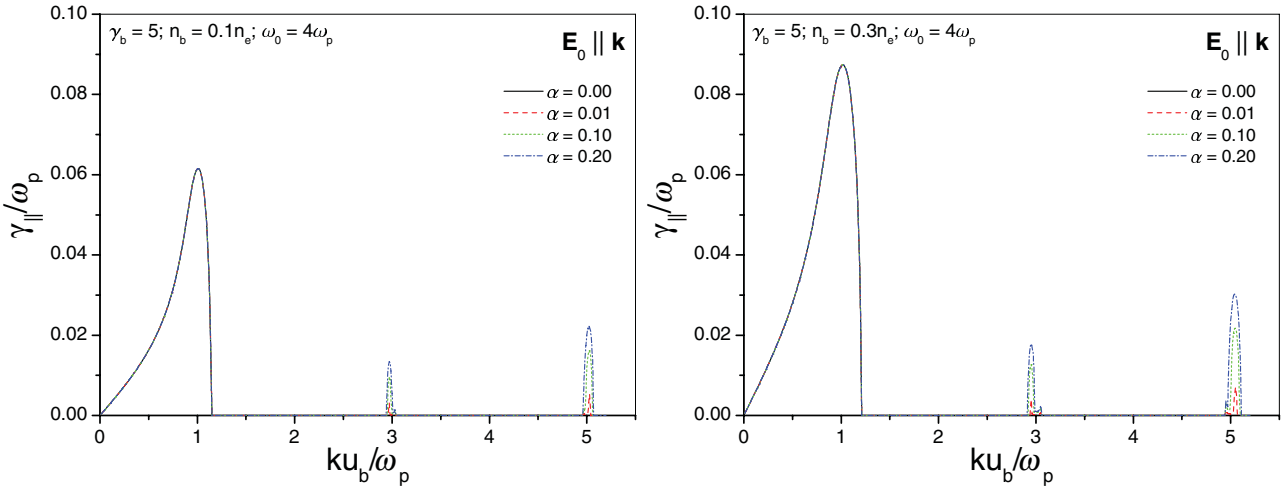

FIG. 5. (Color online) Same as in Fig. 4 but for $\omega_0 = 4\omega_p$, $n_b = 0.1n_e$ (left panel), and $n_b = 0.3n_e$ (right panel).

electromagnetic response of the system is derived in terms of the conductivity tensor of the system involving all harmonics of the RF. After a general introduction to the theoretical model in Sec. II, the dispersion relations of the modes are considered in Secs. III and IV. It is shown that, in general, the longitudinal and transversal modes are parametrically coupled due to the presence of the RF. As a result, the dispersion equation of the modes represents a secular equation for each harmonic of the electromagnetic field. Assuming, however, nonrelativistic laser intensities in Secs. IV and V, we have considered only the lowest (zero, first, and second) harmonics of the fields truncating the secular dispersion equation on the second order of the amplitude of the RF. The dispersion equations derived in these sections led to a detailed presentation, in Sec. VI, of a collection of data through figures on the growth rates. For numerical calculations we have chosen $\gamma_b = 5$, which pertains to the FIS relativistic electron beam in the typical 1- to 2-MeV energy range of practical interest.

Explicit calculations have been done within the cold-fluid approximation, both for the beam and the plasma, neglecting the low-frequency dynamics of the plasma ions. Furthermore, the beam drift velocity is parallel to the wave vector $\mathbf{k}$ of the excitations. Two particular cases of the transverse ($\mathbf{E}_0 \perp \mathbf{k}$) and the longitudinal ($\mathbf{E}_0 \parallel \mathbf{k}$) polarizations of the RF have been studied in detail in Secs. IV and V, respectively. For the longitudinal and the transversal unstable modes we have identified some domains in the ω-k plane corresponding to the resonant and the nonresonant instabilities occurring due to the parametric coupling of the different modes. Analytical expressions for the relevant growth rates have been derived which are well supported by our numerical calculations in Sec. VI. These analytical results go beyond those obtained previously in Refs. [43–45] (see also Refs. [37,38]) and in Refs. [14–16] for the purely parametric and the beam-plasma unstable modes, respectively. In the course of this study, we have also derived, in Appendix C, a dynamical equation for the complex amplitude of the excited modes in $\mathbf{E}_0 \parallel \mathbf{k}$ configuration without any restriction on the number of harmonics. When the initial conditions are specified, this equation may be useful in analyzing the beam-plasma parametric instabilities beyond a weak RF limit considered here.

It was shown that, in the case of the transverse $\mathbf{E}_0 \perp \mathbf{k}$ polarization of the RF, the longitudinal and the transversal modes are coupled due to the RF and can be unstable. The purely beam-plasma and the parametric unstable modes are only weakly coupled in this case. With increasing the laser frequency ω_0 the new branches of the parametrically unstable modes are excited. Furthermore, as demonstrated in Figs. 1–3, the growth rates of these modes (as well as the corresponding domain in the k space) essentially increase with ω_0 and the laser intensity and exceed the growth rate γ^{TS} of the standard two-stream instability. In the case of the parallel polarization (with $\mathbf{E}_0 \parallel \mathbf{k}$), the longitudinal and the transversal modes are decoupled and the instability occurs mainly for the former modes. The purely beam-plasma and the parametric unstable modes are now strongly coupled and the whole instability domain in the k space is split (at $\omega_0 > 2\omega_p$) into three major subdomains. In the long-wavelength subdomain with $0 < k < k_c$ the instability is similar to the two-stream one while at $ku_b \simeq \omega_0 \pm \omega_p$ the instability essentially depends on both the beam and the RF parameters (see Figs. 4 and 5). Finally, it was shown that the growth rates are larger in the case of the transversal polarization $\mathbf{E}_0 \perp \mathbf{k}$ of the laser field.

Going beyond the present approach, which is based on several approximations and assumptions, we can envisage a number of improvements. These include (i) the effects of the low-frequency dynamics of the plasma ions which are completely neglected here, provided that the obtained frequencies are much higher than the ionic frequencies, and (ii) thermal effects both for the beam and the plasma. In principle, in the case of a standard beam-plasma instability the growth rate can be reduced by these effects [28]. However, in the case of a relativistic beam, the thermal momentum spreads of the beam particles in the directions parallel or transverse to the beam velocity has only little influence on the instability [19]. Therefore, these effects are important in the case of the nonrelativistic beams as, for instance, in the experiments with heavy ion beams interacting with a laser irradiated plasma [30–32], and (iii) in studying the influence of the finite sizes of the beam in the longitudinal and the transversal directions on the instability. An expected effect is the self-consistent generation of the counterstreaming current in a plasma [13] which is neglected in the present study. However, this is not a principal restriction on our treatment and the return current can be included by adding into Eqs. (29) and (30) the similar terms but with the flow velocity $\mathbf{u}_e$ [14–16]. The latter is determined from the condition of the beam current neutralization, $n_e\mathbf{u}_e \simeq -n_b\mathbf{u}_b$. (iv) Another important issue not considered here is the effect of the RF on the dynamics of the beam particles. This implies either relativistic beams (with $\gamma_b \gg 1$) or nonrelativistic beams of heavy particles (heavy ions, protons, antiprotons, etc.), (v) considering the contributions of the higher harmonics with $\ell \geqslant 2$. From the structures of Eqs. (38), (39), and (68)–(70), it follows that, in this case, the combined frequencies $\ell\omega_0 \pm \omega_p$ come into play, determining some new branches for the unstable modes. In principle, the study of the generation of the higher harmonics of these modes could be facilitated, employing a dynamical equation for the complex amplitude similar to Eq. (C6) and, (vi) last, studying some other orientations of the polarization vector $\mathbf{E}_0$ of the RF and the beam drift velocity $\mathbf{u}_b$ with respect to $\mathbf{k}$. However, in general, the simultaneous investigation of these issues is a formidable task and requires several separate investigations. We intend to address these issues in our forthcoming investigations.

ACKNOWLEDGMENTS

H.B.N. is grateful for the financial support of the Université Paris–Sud XI, Orsay, and thanks the staff of the Plasma Physics Laboratory for their hospitality during his visit. The work of H.B.N. has been partially supported by the State Committee of Science of the Armenian Ministry of Higher Education and Science (Project No. 11–1c317).

APPENDIX A: BEAM-PLASMA MODES IN A COLD-FLUID APPROXIMATION

In this Appendix, in a cold-fluid model, we briefly consider the asymptotic behavior of the frequencies and the growth

rates of the standard (in the absence of the RF, $v_E = 0$) beam-plasma longitudinal modes at large and small k. A similar qualitative analysis have been conducted in Ref. [28]. We look for the solutions of the dispersion equation $\mathcal{D}_\parallel(k,\omega) = 0$ of the longitudinal modes in the form $\omega = \omega_r + i\gamma$, where ω_r is the (real) frequency and γ is the growth rate of the modes, respectively. Here the dispersion function $\mathcal{D}_\parallel(k,\omega)$ is determined by Eq. (31) with Eqs. (30) and (42).

As mentioned in Sec. IV A, at short wavelengths, $k \geqslant k_c$, there are four real solutions [i.e., $\gamma(k) = 0$] of the dispersion equation which at $k \geqslant k_c$ asymptotically behave as

$$\omega_{r1}^{\pm}(k) = \pm\omega_p\left[1 + \frac{\xi\omega_p^2}{2\gamma_b^3(ku_b)^2} \pm \frac{\xi\omega_p^3}{\gamma_b^3(ku_b)^3} + \cdots\right], \quad \text{(A1)}$$

$$\omega_{r2}(k) = ku_b\left[1 - \frac{\sqrt{\xi}\omega_p}{\gamma_b^{3/2}ku_b} - \frac{\sqrt{\xi}\omega_p^3}{2\gamma_b^{3/2}(ku_b)^3} + \cdots\right], \quad \text{(A2)}$$

$$\omega_{r3}(k) = ku_b\left[1 + \frac{\sqrt{\xi}\omega_p}{\gamma_b^{3/2}ku_b} + \frac{\sqrt{\xi}\omega_p^3}{2\gamma_b^{3/2}(ku_b)^3} + \cdots\right]. \quad \text{(A3)}$$

The modes with the frequencies $\omega_{r3}(k)$ and $\omega_{r1}^-(k)$ remain stable also at $0 \leqslant k < k_c$ while the other mode with $\omega_{r1}^+(k)$ at $k = k_c$ merges with the mode $\omega_{r2}(k)$. The latter becomes unstable at $k < k_c$. The frequency and the growth rate of this mode in this long-wavelength limit ($k < k_c$) asymptotically behave as

$$\omega_{r2}(k) = \frac{ku_b}{1 + \xi/\gamma_b^3}\left[1 + \frac{4\xi\left(1 - \xi/\gamma_b^3\right)}{\gamma_b^3\left(1 + \xi/\gamma_b^3\right)^3}\frac{(ku_b)^2}{\omega_p^2} + \cdots\right], \quad \text{(A4)}$$

$$\gamma(k) = ku_b\frac{\left(\xi/\gamma_b^3\right)^{1/2}}{1 + \xi/\gamma_b^3} \times\left[1 + \frac{1 - 6\xi/\gamma_b^3 + \xi^2/\gamma_b^6}{\left(1 + \xi/\gamma_b^3\right)^3}\frac{(ku_b)^2}{\omega_p^2} + \cdots\right]. \quad \text{(A5)}$$

Similarly, one finds the asymptotic behavior of the stable modes $\omega_{r1}^-(k)$ and $\omega_{r3}(k)$ at $k < k_c$,

$$\begin{pmatrix}\omega_{r1}^-(k)\\ \omega_{r3}(k)\end{pmatrix} = \mp\omega_p\sqrt{1 + \xi/\gamma_b^3}\left[1 \mp \frac{\xi/\gamma_b^3}{\left(1 + \xi/\gamma_b^3\right)^{3/2}}\frac{ku_b}{\omega_p} + \frac{3\xi/\gamma_b^3}{2\left(1 + \xi/\gamma_b^3\right)^3}\frac{(ku_b)^2}{\omega_p^2} + \cdots\right]. \quad \text{(A6)}$$

It is seen that the leading terms in Eqs. (A4) and (A5) coincide with $\omega_\parallel^{\mathrm{TS}}(k)$ and $\gamma^{\mathrm{TS}}(k)$, respectively, see Eq. (44).

APPENDIX B: EVALUATION OF THE SUM

In this Appendix, within the fluid approximation we briefly derive an analytic expression for the function $\Psi_\ell(\zeta)$ introduced in Sec. V [see Eq. (69)]. Inserting Eq. (42) into Eq. (69), we arrive at

$$\Psi_\ell(\zeta) = (-1)^\ell\frac{\omega_p}{2\omega_0}\sum_{s=-\infty}^{\infty}\left(\frac{1}{s + a_+} - \frac{1}{s + a_-}\right)J_s(\zeta)J_{s+\ell}(\zeta), \quad \text{(B1)}$$

where $a_\pm = (\omega \pm \omega_p)/\omega_0$. The summation in Eq. (B1) can be easily done using the Newberger's summation formula [46] which is valid for noninteger μ, $0 \leqslant \gamma \leqslant 1$ and $\mathrm{Re}(\alpha + \beta) > -1$,

$$\sum_{n=-\infty}^{\infty}(-1)^n\frac{J_{\alpha-\gamma n}(\zeta)J_{\beta+\gamma n}(\zeta)}{n + \mu} = \frac{\pi}{\sin(\pi\mu)}J_{\alpha+\gamma\mu}(\zeta)J_{\beta-\gamma\mu}(\zeta). \quad \text{(B2)}$$

In general, μ, α, and β are complex quantities. Using the summation formula (B2) from Eq. (B1) at $\ell \geqslant 0$ and $\ell \leqslant 0$, we obtain

$$\Psi_\ell(\zeta) = (-1)^\ell\frac{\pi\omega_p}{2\omega_0}\left[\frac{1}{\sin(\pi a_+)}J_{a_+}(\zeta)J_{\ell-a_+}(\zeta) - \frac{1}{\sin(\pi a_-)}J_{a_-}(\zeta)J_{\ell-a_-}(\zeta)\right], \quad \text{(B3)}$$

$$\Psi_\ell(\zeta) = \frac{\pi\omega_p}{2\omega_0}\left[\frac{1}{\sin(\pi a_+)}J_{a_+-\ell}(\zeta)J_{-a_+}(\zeta) - \frac{1}{\sin(\pi a_-)}J_{a_--\ell}(\zeta)J_{-a_-}(\zeta)\right], \quad \text{(B4)}$$

respectively.

Consider also the limit of the function $\Psi_\ell(\zeta)$ at small parameter ζ which corresponds to the limit of a weak RF. At $\zeta \ll 1$, using the asymptotic behavior of the Bessel function at small argument [42] from Eqs. (B3) and (B4), we obtain

$$\Psi_\ell(\zeta) = (-1)^{\frac{\ell+|\ell|}{2}}\left(\frac{\zeta}{2}\right)^{|\ell|}\sum_{s=0}^{|\ell|}\frac{(-1)^s}{s!(|\ell| - s)!}\frac{\delta\varepsilon_\parallel(-\eta_\ell s)}{1 + \delta\varepsilon_\parallel(-\eta_\ell s)} + \mathrm{O}(\zeta^{|\ell|+2}), \quad \text{(B5)}$$

where $\eta_\ell = |\ell|/\ell$.

APPENDIX C: DYNAMICAL EQUATION FOR THE COMPLEX AMPLITUDES

In Sec. V, we have derived the dispersion equation for the plasma modes generated simultaneously by the laser radiation and the REB. For some applications the derivation of a differential equation for the complex amplitude of the excited wave is desirable. We consider here the case of a cold plasma when the partial dielectric function is given by Eq. (42). For deriving the dynamical equation for the amplitude, we insert Eqs. (42) and (69) into Eq. (68) and, using the summation formula (67), we represent the latter in the form

$$E_\parallel(0) = -\sum_{\ell=-\infty}^{\infty}E_\parallel(\ell)\delta\varepsilon_{b\parallel}(-\ell) \times\sum_{s=-\infty}^{\infty}\frac{(\omega - s\omega_0)^2}{(\omega - s\omega_0)^2 - \omega_p^2}J_{s-\ell}(\zeta)J_s(\zeta). \quad \text{(C1)}$$

Now, in both sides of Eq. (C1), we make an inverse Fourier transformation. Then, denoting the time-dependent complex amplitude as $\mathcal{E}(t)$ and using the summation formula [42],

$$\sum_{\ell=-\infty}^{\infty} e^{\pm i\ell\omega_0 t} J_\ell(\zeta) = e^{\pm i\zeta \sin(\omega_0 t)}, \tag{C2}$$

we obtain the equation

$$\mathcal{E}(t)e^{i\zeta \sin(\omega_0 t)} = -\int_{-\infty}^{\infty} d\omega E_\parallel(\omega)\delta\varepsilon_{b\parallel}(\omega) \times \sum_{s=-\infty}^{\infty} \frac{(\omega - s\omega_0)^2}{(\omega - s\omega_0)^2 - \omega_p^2} e^{-i(\omega - s\omega_0)t} J_s(\zeta). \tag{C3}$$

Next, on both sides of Eq. (C3), we apply the differential operator $\partial^2/\partial t^2 + \omega_p^2$,

$$\left(\frac{\partial^2}{\partial t^2} + \omega_p^2\right)[\mathcal{E}(t)e^{i\zeta \sin(\omega_0 t)}] = -\frac{\partial^2}{\partial t^2} e^{i\zeta \sin(\omega_0 t)} \int_{-\infty}^{\infty} \delta\varepsilon_{b\parallel}(\omega) E_\parallel(\omega) e^{-i\omega t} d\omega = \frac{\omega_b^2}{\gamma_b^3} \frac{\partial^2}{\partial t^2} e^{i\zeta \sin(\omega_0 t)} \int_{-\infty}^{\infty} \mathcal{E}(\tau) G_b(\tau - t) d\tau. \tag{C4}$$

In the last part of Eq. (C4) we have used the longitudinal dielectric function of the beam, Eq. (30). Here $G_b(t)$ is the Green function of the electron beam

$$G_b(t) = \frac{1}{2\pi} \int_{-\infty}^{\infty} \frac{e^{i\omega t} d\omega}{(\omega - k u_b + i0)^2}, \tag{C5}$$

where we have introduced the positive infinitesimal $+i0$ which guarantees the causality of the response. An explicit expression for the function $G_b(t)$ can be easily obtained, employing, in Eq. (C5), the contour integration technique. The result reads as $G_b(t) = \Theta(-t) t e^{iku_b t}$, where $\Theta(t)$ is the Heaviside unit-step function. Substituting this result into Eq. (C4), we finally arrive at

$$\left(\frac{\partial^2}{\partial t^2} + \omega_p^2\right)[\mathcal{E}(t)e^{i\zeta \sin(\omega_0 t)}] = \frac{\omega_b^2}{\gamma_b^3} \frac{\partial^2}{\partial t^2} e^{i\zeta \sin(\omega_0 t)} \int_{-\infty}^{t} \mathcal{E}(\tau) e^{iku_b(\tau - t)} (\tau - t) d\tau. \tag{C6}$$

The obtained equation (C6) must be accompanied by the initial conditions. When these conditions are specified, Eq. (C6) represents the evolution of the complex amplitude of the waves excited simultaneously by the RF and the REB in a cold plasma. Note that, in contrast to the dispersion equation (71), Eq. (C6) is also valid for the intensity parameter $\zeta \simeq ka \sim 1$.

[1] D. A. Hammer and N. Rostoker, Phys. Fluids **13**, 1831 (1970).
[2] T. Piran, Rev. Mod. Phys. **76**, 1143 (2004).
[3] M. V. Goldman, Rev. Mod. Phys. **56**, 709 (1984).
[4] L. Arons and E. T. Scharlemann, Astrophys. J. **231**, 854 (1979).
[5] M. E. Dieckmann, Phys. Rev. Lett. **94**, 155001 (2005).
[6] M. Tabak, J. Hammer, M. E. Glinsky, W. L. Kruer, S. C. Wilks, J. Woodworth, E. M. Campbell, M. D. Perry, and R. J. Mason, Phys. Plasmas **1**, 1626 (1994).
[7] C. Deutsch, H. Furukawa, K. Mima, M. Murakami, and K. Nishihara, Phys. Rev. Lett. **77**, 2483 (1996).
[8] C. Ren, M. Tzoufras, F. S. Tsung, W. B. Mori, S. Amorini, R. A. Fonseca, L. O. Silva, J. C. Adam, and A. Heron, Phys. Rev. Lett. **93**, 185004 (2004).
[9] D. Batani, S. D. Baton, M. Manclossi, J. J. Santos, F. Amiranoff, M. Koenig, E. Martinolli, A. Antonicci, C. Rousseaux, M. R. Le Gloahec, T. Hall, V. Malka, T. E. Cowan, J. King, R. R. Freeman, M. Key, and R. Stephens, Phys. Rev. Lett. **94**, 055004 (2005).
[10] M. Tatarakis, F. N. Beg, E. L. Clark, A. E. Dangor, R. D. Edwards, R. G. Evans, T. J. Goldsack, K. W. D. Ledingham, P. A. Norreys, M. A. Sinclair, M.-S. Wei, M. Zepf, and K. Krushelnick, Phys. Rev. Lett. **90**, 175001 (2003).
[11] R. A. Fonseca, L. O. Silva, J. W. Tonge, W. B. Mori, and J. M. Dawson, Phys. Plasmas **10**, 1979 (2003).
[12] L. O. Silva, R. A. Fonseca, J. W. Tonge, W. B. Mori, and J. M. Dawson, Phys. Plasmas **9**, 2458 (2002).
[13] M. Honda, J. Meyer-ter-Vehn, and A. Pukhov, Phys. Rev. Lett. **85**, 2128 (2000).
[14] A. Bret, M.-C. Firpo, and C. Deutsch, Phys. Rev. E **70**, 046401 (2004).
[15] A. Bret, M.-C. Firpo, and C. Deutsch, Phys. Rev. E **72**, 016403 (2005).
[16] A. Bret and C. Deutsch, Phys. Plasmas **13**, 042106 (2006).
[17] A. Bret, M.-C. Firpo, and C. Deutsch, Phys. Rev. Lett. **94**, 115002 (2005).
[18] A. Bret, L. Gremillet, D. Bénisti, and E. Lefebvre, Phys. Rev. Lett. **100**, 205008 (2008).
[19] A. Bret, M.-C. Firpo, and C. Deutsch, Laser Part. Beams **24**, 27 (2006).
[20] F. Califano, F. Pegoraro, S. V. Bulanov, and A. Mangeney, Phys. Rev. E **57**, 7048 (1998).
[21] M. Honda, Phys. Rev. E **69**, 016401 (2004).
[22] D. Bohm and E. P. Gross, Phys. Rev. **75**, 1851 (1949); **75**, 1864 (1949).
[23] O. Buneman, Phys. Rev. Lett. **1**, 8 (1958).
[24] B. Fried, Phys. Fluids **2**, 337 (1959).
[25] E. S. Weibel, Phys. Rev. Lett. **2**, 83 (1959).
[26] S. A. Bludman, K. M. Watson, and M. N. Rosenbluth, Phys. Fluids **3**, 747 (1960).
[27] Ya. B. Faĭnberg, V. D. Shapiro, and V. I. Shevchenko, Zh. Eksp. Teor. Fiz. **57**, 966 (1970); Sov. Phys. JETP **30**, 528 (1970).
[28] A. B. Mikhailovskii, *Theory of Plasma Instabilities*, Vol. 1 (Consultant Bureau, New York, 1974).
[29] A. B. Mikhailovskii, *Electromagnetic Instabilities in an Inhomogeneous Plasma* (IOP, Bristol, 1992).
[30] C. Stöckl, O. B. Frankenheim, M. Roth, W. Suß, H. Wetzler, W. Seelig, M. Kulish, M. Dornik, W. Laux, P. Spiller, M. Stetter, S. Stöwe, J. Jacoby, and D. H. H. Hoffmann, Laser Part. Beams **14**, 561 (1996).

[31] M. Roth, T. E. Cowan, M. H. Key, S. P. Hatchett, C. Brown, W. Fountain, J. Johnson, D. M. Pennington, R. A. Snavely, S. C. Wilks, K. Yasuike, H. Ruhl, P. Pegoraro, S. V. Bulanov, E. M. Campbell, M. D. Perry, and H. Powell, Phys. Rev. Lett. **86**, 436 (2001).

[32] A. Frank, A. Blazevic, K. Harres, D. H. H. Hoffmann, R. Knobloch-Maas, F. Nurnberg, A. Pelka, G. Schaumann, M. Schollmeier, A. Schokel, D. Schumacher, J. Schutrumpf, T. Hessling, P. G. Kuznetsov, V. V. Vatulin, O. A. Vinokurov, G. Schiwietz, P. L. Grande, and M. Roth, Phys. Rev. E **81**, 026401 (2010).

[33] E. A. Akopyan, H. B. Nersisyan, and H. H. Matevosyan, Radiophys. Quantum Electrons. **40**, 823 (1997).

[34] H. B. Nersisyan and E. A. Akopyan, Phys. Lett. A **258**, 323 (1999).

[35] H. B. Nersisyan and C. Deutsch, Laser Part. Beams **29**, 389 (2011).

[36] Z.-H. Hu, Y.-H. Song, Z. L. Mišković, and Y.-N. Wang, Laser Part. Beams **29**, 299 (2011).

[37] V. P. Silin, *Parametric Effect of High-Intensity Radiation on Plasmas* (Nauka, Moscow, 1973) (in Russian).

[38] A. F. Alexandrov, L. S. Bogdankevich, and A. A. Rukhadze, *Principles of Plasma Electrodynamics* (Springer, Heidelberg, 1984).

[39] S. Ichimaru, *Basic Principles of Plasma Physics* (W. A. Benjamin, Reading, MA, 1973).

[40] P. Clemmow and J. Dougherty, *Electrodynamics of Particles and Plasmas* (Addison-Wesley, Reading, MA, 1990).

[41] R. C. Davidson, in *Handbook of Plasma Physics*, edited by M. N. Rosenbluth and R. Z. Galeev, Vol. 1 (North-Holland, Amsterdam, 1983).

[42] I. S. Gradshteyn and I. M. Ryzhik, *Table of Integrals, Series and Products* (Academic Press, New York, 1980).

[43] Yu. M. Aliev, V. P. Silin, and C. Watson, Zh. Eksp. Teor. Fiz. **50**, 943 (1966); Sov. Phys. JETP **23**, 626 (1966).

[44] L. M. Gorbunov and V. P. Silin, Zh. Eksp. Teor. Fiz. **49**, 1973 (1965); Sov. Phys. JETP **22**, 1347 (1966).

[45] Yu. M. Aliev and V. M. Bychenkov, Zh. Eksp. Teor. Fiz. **76**, 1586 (1979); Sov. Phys. JETP **49**, 805 (1979).

[46] B. S. Newberger, J. Math. Phys. **23**, 1278 (1982); **24**, 2250 (1983).